

Multiple origins of zircons in jadeitite

Bin Fu · John W. Valley · Noriko T. Kita ·
Michael J. Spicuzza · Chad Paton · Tatsuki Tsujimori ·
Michael Bröcker · George E. Harlow

Received: 17 May 2009 / Accepted: 5 October 2009 / Published online: 24 October 2009
© Springer-Verlag 2009

Abstract Jadeitites form from hydrothermal fluids during high pressure metamorphism in subduction environments; however, the origin of zircons in jadeitite is uncertain. We report ion microprobe analyses of $\delta^{18}\text{O}$ and Ti in zircons, and bulk $\delta^{18}\text{O}$ data for the jadeitite whole-rock from four terranes: Osayama serpentinite mélange, Japan; Syros mélange, Greece; the Motagua Fault zone, Guatemala; and the Franciscan Complex, California. In the Osayama jadeitite, two texturally contrasting groups of zircons

are identified by cathodoluminescence and are distinct in $\delta^{18}\text{O}$: featureless or weakly zoned zircons with $\delta^{18}\text{O} = 3.8 \pm 0.6\%$ (2 SD, VSMOW), and zircons with oscillatory or patchy zoning with higher $\delta^{18}\text{O} = 5.0 \pm 0.4\%$. Zircons in phengite jadeitite from Guatemala and a jadeitite block from Syros have similar $\delta^{18}\text{O}$ values to the latter from Osayama: Guatemala zircons are $4.8 \pm 0.7\%$, and the Syros zircons are $5.2 \pm 0.5\%$ in jadeitite and $5.2 \pm 0.4\%$ in associated omphacite, glaucophanite and chlorite-actinolite rinds. The $\delta^{18}\text{O}$ values for most zircons above fall within the range measured by ion microprobe in igneous zircons from oxide gabbros and plagiogranites in modern ocean crust ($5.3 \pm 0.8\%$) and measured in bulk by laser fluorination of zircons in equilibrium with primitive magma compositions or the mantle ($5.3 \pm 0.6\%$). Titanium concentrations in these zircons vary between 1 and 19 ppm, within the range for igneous zircons worldwide. Values of $\delta^{18}\text{O}$ (whole-rock) $\cong \delta^{18}\text{O}$ (jadeite) and vary from 6.3 to 10.1‰ in jadeitites in all four areas.

These values of $\delta^{18}\text{O}$ and Ti are higher than predicted for hydrothermal zircons, and the $\delta^{18}\text{O}$ values of most zircons are not equilibrated with the coexisting jadeite at reasonable metamorphic temperatures. We conclude that while some zircons may be hydrothermal in origin, a majority of the zircons studied are best explained as relic igneous crystals inherited from precursor rocks; they were not precipitated directly from hot aqueous fluids as previously assumed. Therefore, U–Pb ages from these zircons may date magmatic crystallization and do not establish the timing of high pressure metamorphism or hydrothermal activity.

Communicated by J. Hoefs.

Electronic supplementary material The online version of this article (doi:10.1007/s00410-009-0453-y) contains supplementary material, which is available to authorized users.

B. Fu · J. W. Valley · N. T. Kita · M. J. Spicuzza
WiscSIMS, Department of Geology and Geophysics,
University of Wisconsin, Madison, WI 53706-1692, USA

Present Address:

B. Fu (✉) · C. Paton
School of Earth Sciences, The University of Melbourne,
Parkville, VIC 3010, Australia
e-mail: binfu@unimelb.edu.au

T. Tsujimori
Pheasant Memorial Laboratory,
Institute for Study of the Earth's Interior,
Okayama University, Misasa, Tottori 682-0193, Japan

M. Bröcker
Institut für Mineralogie, Universität Münster,
48149 Münster, Germany

G. E. Harlow
Department of Earth and Planetary Sciences,
American Museum of Natural History,
New York, NY 10024-5192, USA

Keywords Zircon · Jadeite · Hydrothermal ·
Oxygen isotopes · SIMS · Greece · Japan · Guatemala ·
California

Introduction

Jadeitites are rocks rich in jadeite that precipitated from hydrothermal fluids (mostly $\leq 450^\circ\text{C}$) either in veins or as metasomatic replacement of metamorphosed precursors at blueschist or eclogite facies within subduction complexes (Harlow et al. 2007 and references therein). The generally agreed upon hydrothermal genesis of jadeitites has led many to assume that their constituent minerals, including zircon, have a similar origin, and this hypothesis is supported by observations that are reported for some zircons including metamorphic mineral inclusions and trace element compositions (Tsujimori et al. 2005; Bröcker and Keasling 2006). These results have further been interpreted to indicate that geochronology of the zircons dates high pressure (HP) metamorphism. However, we show that not all zircons in jadeitite have these characteristics. Zircons are highly resistant to alteration under hydrothermal or high grade metamorphic conditions (Valley 2003; Page et al. 2007a), and thus it is possible that zircons in jadeitite could be inherited from pre-metamorphic protoliths. Zircons are increasingly recognized as primary igneous minerals in ocean crust (Grimes et al. 2007, 2009a, b; Cavosie et al. 2009), suggesting that many jadeitite zircons could be inherited from igneous rocks that were subducted and metasomatically replaced, and that these zircons date the time of magmatic crystallization at the Mid-ocean ridge. These zircons help constrain the formation and subduction history of ocean crust, and fluid-rock interactions during hydrothermal seafloor alteration and/or during the time period of subduction.

In this study, we report values of $\delta^{18}\text{O}$ and Ti measured in situ by ion microprobe from 10 μm spots on single zircons and values of $\delta^{18}\text{O}$ measured in bulk from host jadeitites. Our investigation builds on previous studies of jadeitite zircons from the same samples, which proposed a hydrothermal/metasomatic origin. The new geochemical data are compared to compositions of igneous zircons from likely protoliths and to predicted compositions for hydrothermal zircons in order to test whether they crystallized during magmatic crystallization or later HP metamorphism. We conclude that many of the zircons studied were not precipitated from aqueous fluids as previously assumed and are best explained as relic igneous crystals inherited from pre-metamorphic igneous protoliths.

Sample descriptions

Jadeitite was studied from four well-documented areas: (1) Osayama, SW Japan (Tsujimori et al. 2005); (2) Syros, Greece (Bröcker and Keasling 2006); (3) the Motagua Fault zone, Guatemala (Harlow et al. 2004); (4) New Idria

in the Franciscan Complex, California (Coleman 1961; Tsujimori et al. 2007). Despite a thorough search, no zircons were found in our samples of the New Idria jadeitite veins or immediate blueschist host rock. Nevertheless, we report new whole-rock oxygen isotope results for early jadeitite and late albite veins and associated host rocks collected for this work; these are useful for comparative purposes. The investigated samples and geochronology of selected localities are described in detail in Electronic supplementary material (ESM) S1.1; we give a brief summary on zircons below.

Two types of zircon in jadeitite have been identified from Osayama, SW Japan, by Tsujimori et al. (2005) based on cathodoluminescence (CL) imaging and ion microprobe U–Pb dating. The ig-type zircons (i.e., Type II of Tsujimori et al. 2005) have zircon cores with concentric, oscillatory or patchy CL zoning (Fig. 4 of Tsujimori et al. 2005) and relatively high Th/U ratios from 0.73 to 0.83, and give an average U–Pb age of 507 ± 39 Ma ($n = 3$). The h-type zircons (i.e., Type I of Tsujimori et al. 2005) occur as entire zircon crystals or rimming ig-type zircons, and show featureless or weak CL zoning (see Fig. 4 of Tsujimori et al. 2005). H-type zircons have lower Th/U ratios mostly between 0.19 and 0.57, and yield an average U–Pb age of 479 ± 44 Ma (2 SD, $n = 25$). In a thin section of Osayama jadeitite, one zircon that is believed to be h-type based on its CL pattern contains inclusions of rutile and jadeite (see Fig. 2 of Tsujimori et al. 2005). Both ig-type and h-type zircons are interpreted to be hydrothermal by Tsujimori et al. (2005).

Zircons from a jadeitite block and associated metasomatic alteration rinds (omphacitite, glaucophanite and chlorite-actinolite schist) from Syros, Greece, have been studied by Bröcker and Keasling (2006). Most of the zircons display regular oscillatory or sector zoning, or homogenous featureless domains. The zircons from this suite of mélange samples as well as from a vein-fractured metabasic host rock (M. Bröcker, unpublished data) yield $^{206}\text{Pb}/^{238}\text{U}$ ages of 79.6 to 79.8 Ma, and are proposed to have formed from hydrothermal fluids during HP metamorphism (Bröcker and Keasling 2006).

Zircons from the Guatemalan phengite jadeitite sample MVE02-8-6 are ~ 70 to 100 μm in size and display regular oscillatory or sector zoning, or homogenous featureless domains (see Fig. S1.1). There is no obvious core-rim texture as commonly seen in HP metamorphic rocks.

Analytical methods

Bulk oxygen isotope analyses of whole-rock, jadeite and albite separates were performed at the University of Wisconsin, Madison, by laser fluorination as described by

Table 1 Comparison of texture and chemistry for zircons from jadeitite from Osayama, SW Japan; Syros, Greece; and Guatemala

	Osayama, SW Japan	Osayama, SW Japan	Syros, Greece	Guatemala
Lithology	Jadeitite	Jadeitite	Jadeitite	Phengite jadeitite
Type of zircon	h-type	ig-type		
Size of crystals	~1 mm	~1 mm	~150–200 μm	<100 μm
Morphology	Euhedral	Sub-euhedral	Euhedral	Euhedral
CL texture	Featureless or weakly zoned	Oscillatory or concentric zones	Concentric or sector zones	Oscillatory zones
Mineral inclusions	Jadeite, rutile	Not observed	Not observed	Rare, not identified
Fluid inclusions	Not observed	Not observed	Not observed	Not observed
Th (ppm)	1.2 to 37, and 81 ($n = 35$)	45 to 68 ($n = 3$)	5 to 1,096 ($n = 15$)	18 to 5,900 ($n = 5$)
U (ppm)	6.4 to 94, and 149 ($n = 35$)	64 to 85 ($n = 3$)	16 to 737 ($n = 15$)	120 to 2,290 ($n = 5$)
Th/U (ratio)	0.19 to 0.57, and 1.20	0.73 to 0.83	0.32 to 1.54	0.04 to 2.57
U–Pb age (Ma)	531 to 370 ($n = 35$)	527 to 488 ($n = 3$)	77 to 83 ($n = 15$)	154 ($n = 8$)
$\delta^{18}\text{O}$ (‰) range	3.2 to 4.4	4.6 to 5.4	4.6 to 5.5	3.9 to 5.4
Average (± 2 SD)	3.8 ± 0.6 ($n = 95$)	5.1 ± 0.4 ($n = 28$)	5.2 ± 0.5 ($n = 28$)	4.8 ± 0.8 ($n = 21$)
$\Delta^{18}\text{O}_{\text{Jd-Zrc}}$ (‰)	4.0 or 5.7	2.8 or 4.4	1.8	2.5
$\epsilon_{\text{Hf}}(t)$	~+10	~+7	n.d.	n.d.
REE total (ppm)	75 to 340	460 to 640	n.d.	2,950 to 6,400
(Sm/La) _N	4 to 120	86 to 144	n.d.	205 to 4,461
Ce/Ce*	6 to 46	62 to 77	n.d.	15 to 409
Eu/Eu*	0.64 to 1.30	0.63 to 0.71	n.d.	0.07 to 0.45
Ti (ppm)	2.3 to 7.8 ($n = 12$)	1.0 to 3.2 ($n = 14$)	4.2 to 14 ($n = 22$)	4.5 to 19 ($n = 11$)
Origin of zircon	Hydrothermal/metasomatic	Inherited igneous	Inherited igneous	Both inherited and hydrothermal

Data sources: Tsujimori et al. (2005), Bröcker and Keasling (2006) and this study. *Jd* jadeite or jadeitite whole rock ($\delta^{18}\text{O}$ values, see Table 2), *Zrc* zircon ($\delta^{18}\text{O}$ values, see Electronic supplementary material S2)

n.d. no data

Valley et al. (1995) and Spicuzza et al. (1998). All $\delta^{18}\text{O}$ values are reported relative to Vienna Standard Mean Ocean Water (VSMOW). Six zircon grains were separated from the Guatemalan phengite jadeitite sample MVE02-8-6 (~2 cm³) that were treated in HF at room temperature for 21 days and handpicked from the residues. The zircons were imaged using a JSM-6360LV scanning electron microscope (SEM) with a Centaurus CL detector at Colgate University before in situ analysis. Ion microprobe analyses of $^{18}\text{O}/^{16}\text{O}$ ratios and trace element (Ti, REEs—rare earth elements, U and Th) concentrations in zircons were made on a CAMECA IMS-1280 ion microprobe at the University of Wisconsin, Madison. Analytical procedures were reported previously (Page et al. 2007b; Kita et al. 2009; Valley and Kita 2009). The locations of ion microprobe pits for oxygen isotopes and Ti concentrations were correlated, when applicable, with the SHRIMP U–Pb pits for the Osayama and Syros zircons. Laser ablation U–Pb and hafnium isotope analyses for the Guatemalan and Osayama zircons, respectively, were carried out (after ion microprobe analyses) at the University of Melbourne, using the 193-nm excimer laser-based HELEX ablation system equipped with two inductively coupled plasma mass spectrometers (ICP-MS) described in Woodhead et al.

(2004), Hellstrom et al. (2008) and Paton et al. (2009; see also ESM S1.2). The results were calibrated with the standard zircons 91500, Temora, BR-266 and KIM-5 (Wiedenbeck et al. 1995; Black et al. 2003a, b, 2004; Woodhead et al. 2004; Cavosie et al. 2005).

Results

The current and existing results for the jadeitite zircons are summarized in Table 1, and whole-rock and mineral oxygen isotope compositions for jadeitites and associated blackwall alteration zones are listed in detail in Table 2. All ion microprobe and ICP-MS results ($^{18}\text{O}/^{16}\text{O}$, Ti, REEs, $^{176}\text{Hf}/^{177}\text{Hf}$, U–Pb) for zircons from Osayama, Japan, Guatemala and Syros, Greece are listed in ESM S2 to S6. The average $\delta^{18}\text{O}$ values for individual zircons are summarized in Table 3.

Osayama, Japan

Whole-rock oxygen isotope ratios of jadeitites from Osayama are relatively high, 7.8 and 9.5‰ (Table 2), considerably above those in fresh igneous rocks from

Table 2 Whole-rock and mineral oxygen isotope ratios of jadeitites and associated rocks analyzed by laser fluorination

Sample	Lithology	$\delta^{18}\text{O}$ (‰) VSMOW	$\delta^{18}\text{O}$ (‰) Average
Osayama, SW Japan			
OSJ-A	Jadeitite WR	9.79, 9.15	9.47
OSJ-B	Jadeitite WR	7.83, 7.77	7.80
Syros, Greece			
3148 (A)	Jadeitite WR	7.69	7.69
3148 (B)	Jadeitite WR	6.30	6.30
3149	Omphacitite WR	5.65	5.65
3150	Glaucophanite WR	6.65	6.65
3152	Chlorite-actinolite schist WR	5.91	5.91
Guatemala			
(A) MVE02-8-6	Jadeitite WR	7.31, 7.31	7.31
	Jadeite (HF, 24 h)	7.32, [7.36], [7.44]	
	Jadeite (HF, 6 days)	[7.49]	
	Jadeite (HF, 21 days)	[7.15], [7.15]	
(B) MVE02-39-6	Jadeitite WR	8.23, 7.97	8.05
	Jadeite (HF, 24 h)	8.12	
	Jadeite (HF, 6 days)	7.89	
New Idria, CA			
NIJ-Ab	Vein Albite	12.24, 12.11	12.18
NIJ-Jd	Vein Jadeite	10.08	10.08
NIJ-Host	Blueschist WR	10.19, 10.16	10.18

Whole-rock (WR) samples were analyzed by airlock (Spicuzza et al. 1998), except data in brackets performed in normal analysis chamber

modern ocean crust, but consistent with rocks altered by low temperature interaction with seawater (Eiler 2001). Within a single jadeitite hand sample (OSJ-A), whole rock $\delta^{18}\text{O}$ values of 9.2 and 9.8‰ show local heterogeneity at the centimeter scale.

Ion microprobe $\delta^{18}\text{O}$ results for the two morphological types of zircon from the Osayama jadeitites define homogeneous but distinct populations (Fig. 1a): h-type zircon analyses average $3.8 \pm 0.6\text{‰}$ (2 SD, $n = 95$), while ig-type zircons average $5.1 \pm 0.4\text{‰}$ ($n = 28$). The within-type $\delta^{18}\text{O}$ variations are comparable to the analytical precision for the KIM-5 zircon standard analyzed in the same mount (0.6‰, 2 SD, $n = 69$). A few of the Osayama zircon grains show resolvable core versus rim gradients in $\delta^{18}\text{O}$ (e.g., 1.5–2.0‰ for grain no. 11, Fig. 2). The range and spatial distribution seen in these zoned grains ($\delta^{18}\text{O} \sim 5\text{‰}$ in the core vs. $\sim 3.5\text{‰}$ in the rim) mimics the difference between ig-type and h-type zircons found in discrete grains and is correlative with the textural and U–Pb data of Tsujimori et al. (2005).

Titanium concentrations in Osayama zircons vary between 1.0 to 7.8 ppm (average: 3.5 ± 4.1 ppm, 2 SD, $n = 32$; ESM S3 and S4). The average measured Ti concentrations in ig-type and h-type zircons are distinctly different: 2.1 ± 1.5 ppm (2 SD, $n = 12$) versus 4.9 ± 3.9 ppm ($n = 12$) (Fig. 3). Uncorrected Ti-in-zircon

temperatures range from 600 to 700°C (Fig. 3; Watson et al. 2006, but see Fu et al. 2008).

Hafnium isotope ratios ($^{176}\text{Hf}/^{177}\text{Hf}$) are also bimodal and range from 0.282613 ± 29 (2 SE) in the ig-type zircons to 0.282813 ± 35 in the h-type zircons (ESM S5). These ratios correspond to average $\varepsilon_{\text{Hf}}(t)$ values of $+7.2 \pm 3.0$ (2 SE, $n = 4$) in ig-type and $+10.1 \pm 3.6$ ($n = 8$) in h-type zircons (Fig. 4), and to Lu–Hf model ages (T_{DM} ; DM, depleted mantle) of 910 to 750 Ma and 760 to 610 Ma, respectively. A line regressed through most of the data points ($N = 7$; not including one younger outlier, ~ 420 Ma) for h-type zircons in Fig. 4 has a correlation coefficient of 0.83, which suggests a hafnium model age of 570 Ma, coincident with the age of gabbroic dikes from serpentinized peridotites in the same mélangé (~ 560 Ma; Hayasaka et al. 1995).

Syros, Greece

In contrast to Osayama, a single age population of zircons is found in the jadeitite and associated metasomatic reaction rinds from Syros (~ 80 Ma; Bröcker and Keasling 2006). Likewise, CL textures, $\delta^{18}\text{O}$ and Ti of Syros zircons also define a single population (Figs. 1, 3; Table 1). The range in average $\delta^{18}\text{O}$ for all the measured Syros zircon grains is 4.6 to 5.6‰ ($5.2 \pm 0.3\text{‰}$, $n = 46$). Individual

Table 3 Average $\delta^{18}\text{O}$ values (‰VSMOW) for individual zircon grains from jadeitite and associated rocks measured by ion microprobe

Mount_sample_grain	Average $\delta^{18}\text{O}$	± 2 SD	No. spot analyses
Jadeitite, Osayama, SW Japan			
Tsujimori_OSJ_#1 (h-type)	3.46	0.24	($n = 2$)
Tsujimori_OSJ_#3C (ig-type)	5.24	0.35	($n = 3$)
Tsujimori_OSJ_#3R (h-type)	3.91	0.49	($n = 1$)
Tsujimori_OSJ_#5 (h-type)	3.95	0.58	($n = 6$)
Tsujimori_OSJ_#6 (h-type)	3.84	0.39	($n = 6$)
Tsujimori_OSJ_#7 (h-type)	3.69	0.25	($n = 9$)
Tsujimori_OSJ_#8 (ig-type)	5.27	0.10	($n = 5$)
Tsujimori_OSJ_#9 (h-type)	4.07	0.30	($n = 18$)
Tsujimori_OSJ_#10 (h-type)	3.87	0.28	($n = 10$)
Tsujimori_OSJ_#11C (ig-type)	5.04	0.27	($n = 13$)
Tsujimori_OSJ_#11R (h-type)	3.54	0.41	($n = 19$)
Tsujimori_OSJ_#12 (h-type)	3.97	0.32	($n = 2$)
Tsujimori_OSJ_#13 (h-type)	3.44	0.29	($n = 7$)
Tsujimori_OSJ_#14 (h-type)	3.95	0.43	($n = 7$)
Tsujimori_OSJ_#15C (ig-type)	4.85	0.48	($n = 7$)
Tsujimori_OSJ_#15R (h-type)	3.56	0.73	($n = 4$)
Tsujimori_OSJ_#16 (h-type)	4.09	0.11	($n = 3$)
Jadeitite, Guatemala			
WF018_MVE02-8-6_Zrc1	4.90	0.67	($n = 10$)
WF018_MVE02-8-6_Zrc2	4.27	1.16	($n = 2$)
WF018_MVE02-8-6_Zrc3	4.74	0.82	($n = 5$)
WF018_MVE02-8-6_Zrc4	4.45	0.23	($n = 2$)
WF018_MVE02-8-6_Zrc5	5.12	0.25	($n = 2$)
WF018_MVE02-8-6_Zrc6	4.96	0.20	($n = 1$)
Jadeitite, Syros, Greece			
Broecker-1_3148_2	5.29	0.33	($n = 2$)
Broecker-1_3148_4	5.11	0.46	($n = 2$)
Broecker-1_3148_6	5.19	0.41	($n = 3$)
Broecker-1_3148_7	5.11	0.34	($n = 1$)
Broecker-1_3148_8	5.23	0.64	($n = 3$)
Broecker-1_3148_9	4.90	0.34	($n = 2$)
Broecker-1_3148_10	4.62	0.34	($n = 1$)
Broecker-1_3148_12	5.29	0.18	($n = 3$)
Broecker-1_3148_14	5.27	0.18	($n = 2$)
Broecker-1_3148_15A	5.02	0.02	($n = 2$)
Broecker-1_3148_15B	5.37	0.27	($n = 2$)
Broecker-1_3148_16	5.46	0.24	($n = 1$)
Broecker-1_3148_19	5.11	0.41	($n = 2$)
Broecker-1_3148_20	4.98	0.51	($n = 2$)
Omphacitite, Syros, Greece			
Broecker-3_3149_7	5.17	0.48	($n = 3$)
Broecker-3_3149_10	5.16	0.73	($n = 2$)
Broecker-3_3149_15	4.96	0.14	($n = 2$)

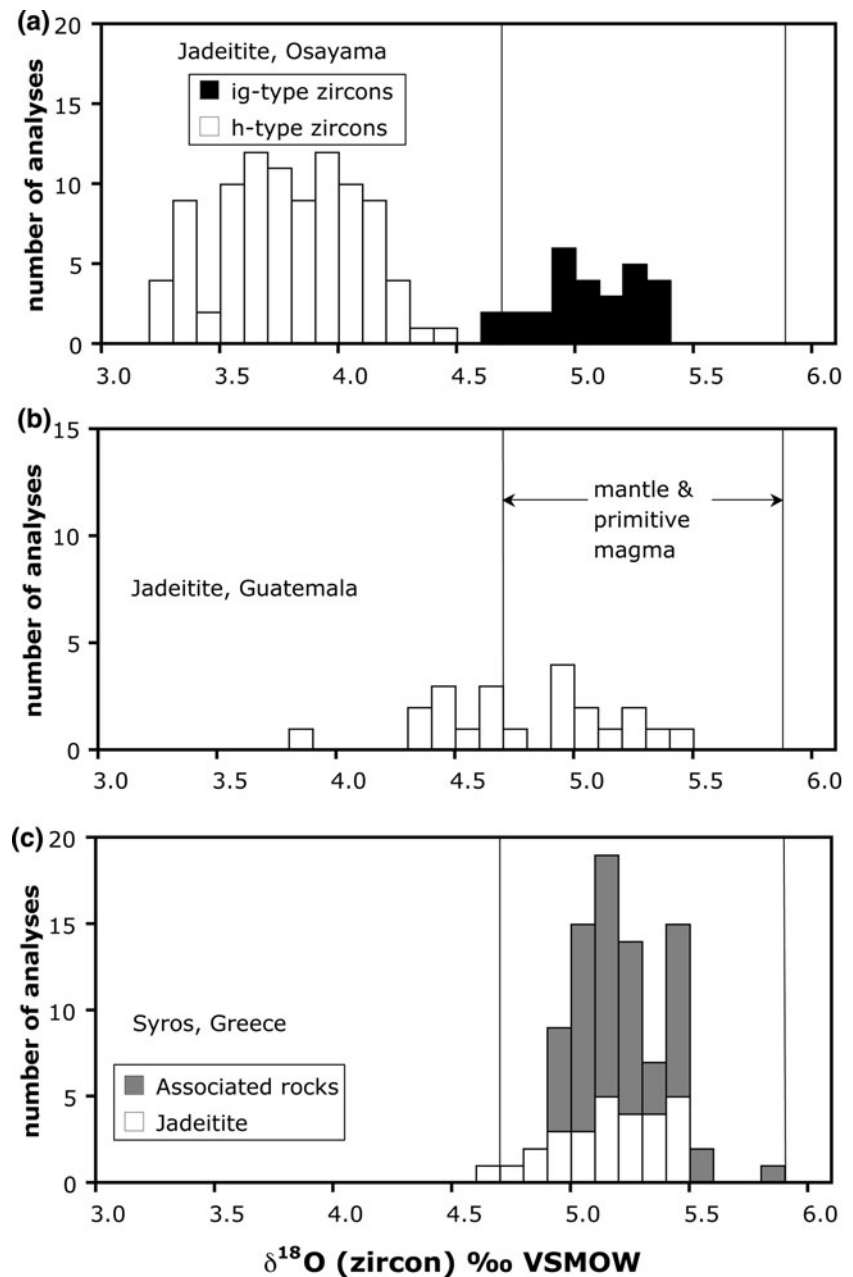
Table 3 continued

Mount_sample_grain	Average $\delta^{18}\text{O}$	± 2 SD	No. spot analyses
Broecker-3_3149_17	5.48	0.22	($n = 1$)
Broecker-3_3149_18	5.09	0.22	($n = 1$)
Broecker-3_3149_19	5.28	0.19	($n = 2$)
Broecker-3_3149_32B	5.62	0.60	($n = 2$)
Glaucofanite, Syros, Greece			
Broecker-3_3151_16A	5.23	0.56	($n = 2$)
Broecker-3_3151_17	5.11	0.06	($n = 2$)
Broecker-3_3151_20	5.24	0.74	($n = 2$)
Broecker-3_3151_6	5.31	0.25	($n = 3$)
Broecker-3_3151_7	5.48	0.10	($n = 2$)
Broecker-3_3151_9	5.23	0.25	($n = 1$)
Chlorite-actinolite schist, Syros, Greece			
Broecker-1_3152A_1	5.40	0.04	($n = 2$)
Broecker-1_3152A_3	5.10	0.20	($n = 1$)
Broecker-1_3152A_4	5.20	0.14	($n = 2$)
Broecker-1_3152A_6A	5.40	0.20	($n = 1$)
Broecker-1_3152A_7	5.14	0.20	($n = 1$)
Broecker-1_3152A_8	5.09	0.20	($n = 1$)
Broecker-1_3152A_11	5.03	0.20	($n = 1$)
Broecker-1_3152A_13	5.07	0.08	($n = 2$)
Broecker-1_3152A_15	5.18	0.34	($n = 3$)
Broecker-1_3152A_17	5.20	0.33	($n = 3$)
Broecker-1_3152A_18	5.29	0.20	($n = 1$)
Broecker-1_3152A_23	5.26	0.40	($n = 2$)
Broecker-3_3152B_3	5.20	0.06	($n = 2$)
Broecker-3_3152B_4A	5.11	0.30	($n = 2$)
Broecker-3_3152B_7	5.04	0.26	($n = 2$)
Broecker-3_3152B_9	5.16	0.07	($n = 2$)
Broecker-3_3152B_9B	5.10	0.27	($n = 1$)
Broecker-3_3152B_12	5.18	0.06	($n = 2$)
Broecker-3_3152B_16	5.02	0.15	($n = 2$)

Spot-to-spot reproducibility (2 SD) of KIM-5 standard during the sessions was typically better than 0.3‰

analyses for zircons from jadeitite average $5.2 \pm 0.5\text{‰}$ (2 SD, $n = 28$), identical to zircons from associated omphacitite, glaucophanite and chlorite-actinolite rinds ($5.2 \pm 0.4\text{‰}$, $n = 58$). Five spot analyses with anomalously low $\delta^{18}\text{O}$ (down to 3.3‰; ESM S2) are omitted from the averages given above. These anomalous values were measured in undated grains or domains showing a disturbed CL pattern similar to the much younger (~ 52 Ma) zircons reported in the same region by Tomaschek et al. (2003). It is possible that these five analysis pits represent domains of crystals that formed in a different manner from the main generation of zircons that were studied here. By comparison, whole-rock $\delta^{18}\text{O}$ for jadeitite and associated

Fig. 1 Histograms of $\delta^{18}\text{O}$ values analyzed by ion microprobe in zircons from jadeitite and associated rocks from **a** Osayama, SW Japan, **b** Guatemala and **c** Syros, Greece. All Syros and many Guatemalan zircons can be grouped with ig-type Osayama zircons and are interpreted in this study to be magmatic (see text). Note that igneous zircons from the mantle and in equilibrium with primitive magmatic compositions have values of $\delta^{18}\text{O} = 5.3 \pm 0.6\text{‰}$ (2 SD; Valley et al. 2005)



blackwall alteration zones in the Syros mélange vary from 5.7 to 7.9‰ (Table 2). At the centimeter scale, jadeitites from both Syros and Osayama vary by over 1.5‰ (Table 2), while the zircons are homogeneous within analytical uncertainty.

Our results are also consistent with laser fluorination results of Katzir et al. (2002) for bulk zircon separates from jadeitite on the island of Tinos, Greece ($\delta^{18}\text{O} = 5.01 \pm 0.01\text{‰}$) and from omphacitite on Syros ($\delta^{18}\text{O} = 5.09 \pm 0.06\text{‰}$, $n = 4$).

Titanium concentrations in the Syros zircons show considerable variability (3.3–16 ppm), and the ranges for zircons from different host rocks are comparable:

4.2–14 ppm (9.5 ± 5.4 ppm, 2 SD, $n = 22$) for zircon from jadeitite and 3.3–16 ppm (8.5 ± 6.8 ppm, $n = 42$) for zircon from associated rocks.

Guatemala

Values of $\delta^{18}\text{O}$ from jadeite mineral separates and jadeitite whole-rock were measured by laser fluorination. In order to concentrate jadeite, samples were leached with HF, and high purity jadeite separates were prepared by hand-picking. The $\delta^{18}\text{O}$ values of jadeite separates are indistinguishable from values for whole-rock samples that were not HF-treated (Table 2).

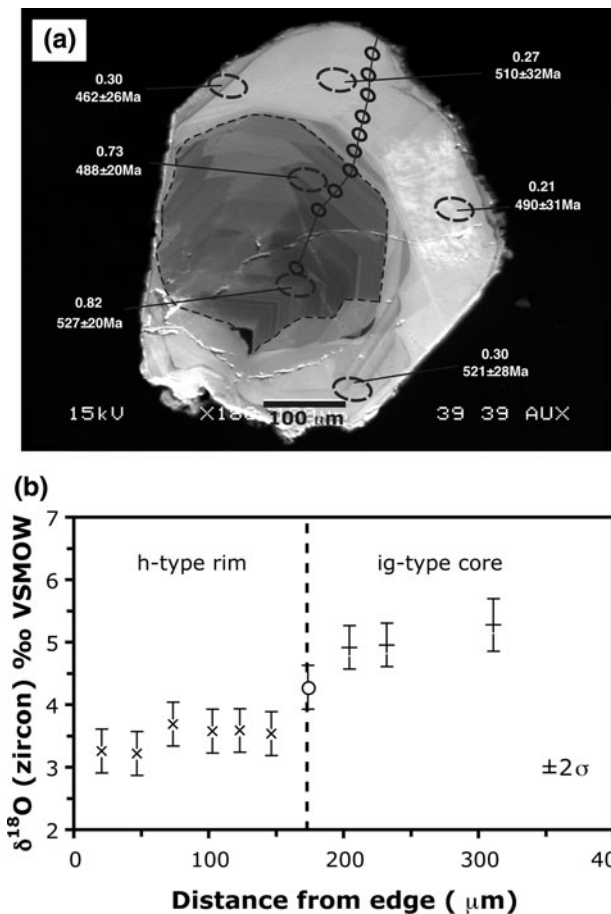


Fig. 2 CL image and oxygen isotope ratios measured in a traverse of a single zircon grain (no. 11, Tsujimori et al. 2005) from Osayama, SW Japan: **a** CL image, *small open symbols* show 10-μm-diameter ion microprobe oxygen isotope pits (many other O-pits are not shown here, see Electronic supplementary materials S2), *large dashed open symbols* show 25-μm U–Pb pits, *numbers* represent Th/U ratios and U–Pb ages (±2 SE), *scale bar* 100 μm; **b** values of $\delta^{18}\text{O}$ from a core to rim traverse along the *solid line* in (a). Note that in this zircon, the core corresponds to ig-type zircon (Th/U > 0.3), and the rim is h-type zircon (Th/U ≤ 0.3) after Tsujimori et al. (2005), respectively. Ig-type zircon crystallized before h-type zircon, although U–Pb ages are indistinguishable within uncertainty of ±38 Myr (2 SE)

Zircon oxygen isotope and trace element data were obtained for the Quebrada El Silencio phengite jadeitite. Values of $\delta^{18}\text{O}$ for individual zircons vary from 3.9 to 5.4‰. All spot analyses, if taken together, average $4.8 \pm 0.8\text{‰}$ (2 SD, $n = 22$), and the data are significantly more variable than zircons from Syros (Fig. 1b, ESM S2). Titanium concentrations in these zircons vary between 4.5 and 19 ppm (13 ± 10 ppm, 2 SD, $n = 11$). One measurement of 240 ppm Ti is unreasonably high for terrestrial zircons (mostly ≤20 ppm; Fu et al. 2008) and probably resulted from a Ti-rich inclusion (e.g., rutile).

Laser ablation ICP-MS U–Pb dating of the Quebrada El Silencio zircons yields a single grouping of data points just

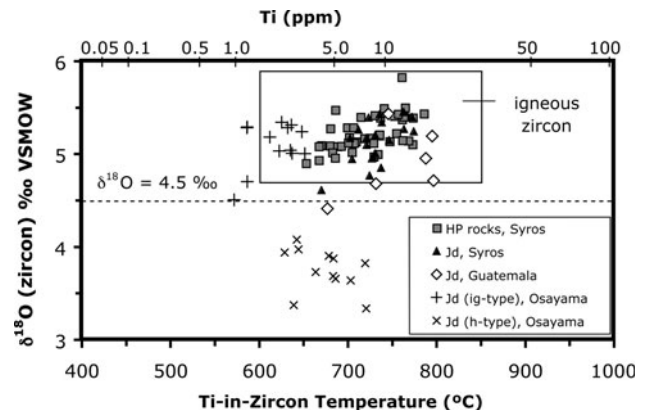


Fig. 3 Apparent Ti-in-zircon temperatures (uncorrected) and Ti concentrations versus $\delta^{18}\text{O}$ (zircon) from jadeitite and associated rocks from Syros, Greece; Guatemala; and Osayama, Japan. The *dashed line* ($\delta^{18}\text{O} = 4.5\text{‰}$) separates Osayama h-type zircons from ig-type zircons. Note that igneous zircons worldwide are shown by the *box*: values of $\delta^{18}\text{O}$ in equilibrium with mantle compositions are $5.3 \pm 0.6\text{‰}$ (2 SD; Valley et al. 2005) and apparent temperatures range from 600 to 850°C (Fu et al. 2008)

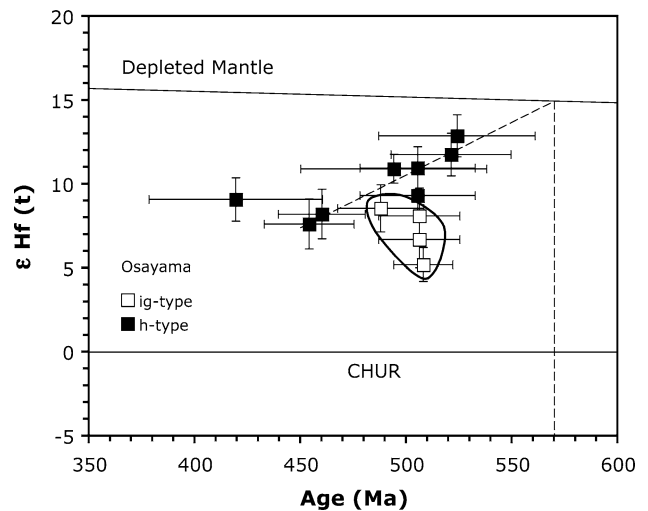


Fig. 4 Initial epsilon hafnium values of zircon ($\epsilon_{\text{Hf}}(t)$) versus in situ ion microprobe U–Pb ages from Osayama, SW Japan. The age data are taken from Tsujimori et al. (2005). *Error bars* are 2 standard errors. All data points lie between the CHUR (chondritic uniform reservoir) evolution line of the mantle and a MORB type reservoir, i.e., an increasingly LILE (large ion lithophile element)-depleted mantle. The regression line (*dash*, $R^2 = 0.83$) is defined by h-type zircons excluding one outlier and corresponds to the Hf isotopic evolution of source (or parent) igneous rocks extracted from the mantle at 570 Ma

above and overlapping concordia near 154 Ma (Fig. 5). After common Pb correction (using a 154-Ma model Pb composition; Stacey and Kramers 1975), the data points yield an average of 153.7 ± 3.5 Ma (2 SD, 8 out of 9 analyses; ESM S6). It appears that only one generation of zircon is present in this phengite jadeitite.

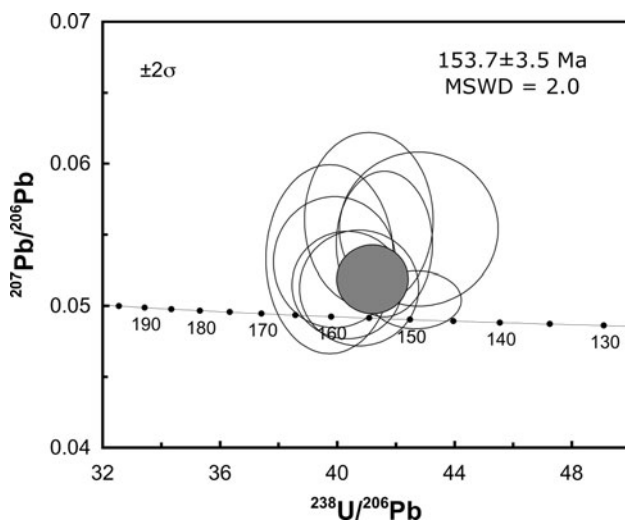


Fig. 5 Terra–Wasserberg concordia diagram of U–Pb for zircons from the Guatemalan phengite jadeitite. The initial common Pb isotopic composition of the zircons was estimated using the two-stage terrestrial Pb evolution model of Stacey and Kramers (1975) at 154 Ma. Data-points error ellipses are 2 SE

Franciscan Formation, New Idria, CA

A late albite vein from New Idria, CA, has a whole-rock $\delta^{18}\text{O} = 12.2\text{‰}$, whereas both an early jadeite vein and the adjacent blueschist have lower, but identical values of $\delta^{18}\text{O}$ (10.1–10.2‰) by laser fluorination.

Discussion

Zircons from igneous rocks

The $\delta^{18}\text{O}$ values of jadeitite zircons from this study can be compared to values found in igneous rocks that are likely protoliths to the jadeitite. The Syros zircons yield a uniform $\delta^{18}\text{O}$ value of $5.2 \pm 0.5\text{‰}$ (2 SD) from 86 analyses in four rocks. Likewise, the $\delta^{18}\text{O}$ values of ig-type zircons in the Osayama jadeitite are constant at $5.0 \pm 0.4\text{‰}$. The Guatemala zircons are more variable and may have formed by more than one process, but still the average is $4.8 \pm 0.8\text{‰}$ with many values above 4.7 (Table 3). These values are mostly identical within analytical uncertainty to those of igneous zircons measured by ion microprobe from oxide gabbros, norites and plagiogranites of modern ocean crust ($5.2 \pm 0.5\text{‰}$; Cavosie et al. 2009; Grimes et al. 2009b) and to igneous zircons measured in bulk by laser fluorination in high temperature equilibrium with primitive magma compositions or the mantle ($5.3 \pm 0.6\text{‰}$; Valley et al. 2005) (Fig. 1a–c).

In contrast to ig-type, the h-type zircons from Osayama average $3.8 \pm 0.6\text{‰}$, which is distinctly lower than normal

igneous zircons. Only a few of the grains from the Osayama jadeitite appear to incorporate both ig-type and h-type zircons. When both types are found in one crystal, the h-type zircon forms the rims and has lower $\delta^{18}\text{O}$ values than the ig-type zircon cores (e.g., zircon no. 11 in Fig. 2). This relation suggests that igneous zircon cores are overgrown by hydrothermal or metamorphic zircon rims.

Compared to the zircons, jadeitite whole-rock $\delta^{18}\text{O}$ values are much more variable. Overall, $\delta^{18}\text{O}$ values of jadeite grains or jadeitite whole rock from Osayama, Guatemala, Syros, and New Idria, CA, vary from 7.0 to 10.1‰. Here, we assume $\delta^{18}\text{O}$ (WR) \cong $\delta^{18}\text{O}$ (jadeite) because the jadeitites consist of over 90 modal percentage jadeite. These data are consistent with published jadeite $\delta^{18}\text{O}$ values of 8.0 to 9.4‰ from Guatemala (Johnson and Harlow 1999). However, these values are higher than whole-rock $\delta^{18}\text{O}$ values of 3.4 to 6.4‰ for meta-gabbros and HP rocks (e.g., omphacitite) from Syros (Putlitz et al. 2000; Katzir et al. 2002), which represent ocean crust that was hydrothermally altered by seawater on an ocean ridge at higher temperatures than the jadeitites of this study. Sorensen et al. (2006) report large (>4‰) variations within individual CL-zoned jadeite crystals in jadeitites from Guatemala, California, SW Japan, Burma and Kazakhstan.

Oxygen isotopic disequilibrium

The fractionation of $\delta^{18}\text{O}$ between zircons and jadeite host rock provides a further test of the processes of formation. If both zircon and jadeite precipitated from the same hydrothermal fluid, they would be expected to be in isotopic equilibrium. These two minerals have slow oxygen diffusion rates and should preserve primary compositions (Valley 2001); in particular, zircons have been demonstrated to be refractory and highly retentive, retaining their magmatic O-isotope values through high-grade metamorphism and intense hydrothermal alteration (Valley 2003; Page et al. 2007a).

The equilibrium oxygen isotope fractionation between jadeite and zircon can be quantified from calibrations of quartz/jadeite and quartz/zircon equilibria (Matthews et al. 1983; Valley et al. 2003):

$$\begin{aligned} \delta^{18}\text{O}_{\text{Jd}} - \delta^{18}\text{O}_{\text{Zrc}} &= \Delta^{18}\text{O}_{\text{Jd-Zrc}} \approx 1000 \cdot \ln(\alpha_{\text{Jd-Zrc}}) \\ &= 1.55 \times 10^6 / T^2 (T \text{ in K}) \end{aligned} \quad (1)$$

Based on this relation, $\Delta^{18}\text{O}_{\text{Jd-Zrc}}$ is 3.0‰ at 450°C and 1.6‰ at 700°C.

The oxygen isotope fractionations measured in jadeitites of this study are highly variable (Table 1); $\Delta^{18}\text{O}_{\text{Jd-Zrc}}$ is: 1.8‰ for the Syros jadeitite, 2.5‰ for the Guatemalan phengite jadeitite, 2.8 or 4.4‰ (ig-type) and 4.0 or 5.7‰

(h-type) for the Osayama jadeitite. If equilibrated, these results would correspond to apparent oxygen isotope temperatures from 655 to 250°C (Eq. 1), indicating that many of the zircons are out of oxygen isotope equilibrium with the coexisting jadeites for metamorphic temperatures of $\leq 450^\circ\text{C}$ (Harlow et al. 2007). However, such estimates are further complicated by heterogeneity of $\delta^{18}\text{O}$ in jadeitite found in this study and by Sorensen et al. (2006). Oxygen isotope fractionations have been measured also for coexisting albite and jadeite. For the New Idria samples, one albite-jadeite pair ($\Delta^{18}\text{O}_{\text{Ab-Jd}} = 2.1\text{‰}$) would indicate an apparent temperature of 257°C, based on the calibration of Matthews et al. (1983). Furthermore, Sorensen et al. (2006) report $\Delta^{18}\text{O}_{\text{Ab-Jd}}$ values ranging from 7.7 to 2.6‰, with apparent temperatures of 6° to 209°C from two samples from Burma. Such low and variable apparent temperatures demonstrate oxygen isotopic disequilibrium conditions for albite and jadeite in these rocks. We note that jadeite in the Burmese samples studied by Sorensen et al. (2006) is in direct contact with albite, while this is not the case at New Idria.

Overall, the oxygen isotope ratios in jadeitite are characterized by variable and high $\delta^{18}\text{O}$ in jadeite crystals, centimeter-size chips of whole rocks and in decimeter-size whole rocks, and an apparent lack of oxygen isotope equilibrium among coexisting minerals. This variability contrasts with the values of $\delta^{18}\text{O}$ for zircons within jadeitites, which are uniformly lower and in most cases fall in the narrow range of 4.5 to 5.5‰. These results suggest that many zircons formed by a different process than jadeite.

Origin of zircons

Most $\delta^{18}\text{O}$ values in zircons in this study (excluding Osayama h-type zircons and possibly some Guatemala zircons) fall within the narrow range of zircon values from oxide gabbros, norites and plagiogranites of modern ocean crust (Cavosie et al. 2009; Grimes et al. 2009b). This fact suggests that these zircons are remnants from the igneous protoliths of jadeitite, or possibly detrital igneous zircons incorporated into the magmas, and that during metasomatic replacement the zircons remained unaffected. In contrast, the $\delta^{18}\text{O}$ values of host jadeitites are more variable and not in isotopic equilibrium, indicating that jadeite formed at a different, presumably later time.

Alternatively, if the uniform compositions of most jadeitite zircons resulted from hydrothermal/metasomatic processes, then it would be necessary that zircon crystallized at a narrow range of temperatures and from fluids, which resulted in a narrow range of values that fortuitously match igneous zircons, while the jadeites are highly variable in $\delta^{18}\text{O}$.

Other lines of evidence for the formation of zircons in jadeitite include chemical compositions, mineral inclusions and geochronology. Firstly, titanium concentrations for all the analyzed zircons, 1 to 19 ppm, are indistinguishable from known igneous zircons (mostly ≤ 20 ppm; Fu et al. 2008). If accurate, the Ti-in-zircon thermometer (Watson et al. 2006; Ferry and Watson 2007) indicates that zircons in phengite jadeitite from Guatemala, which contains quartz and rutile, crystallized at higher temperatures (average 760°C) than the formation of jadeitite (mostly $\leq 450^\circ\text{C}$; Harlow et al. 2007). While application of this thermometer is not fully constrained, especially in other samples that may not contain quartz or rutile, when Ti-in-zircon temperatures are not in agreement, they are generally lower than other independent estimates for crystallization of igneous rocks (Fu et al. 2008; see ESM S1.3).

Secondly, our preliminary trace element results indicate that some zircons from Guatemala and Osayama share similar characters with typical igneous zircons from either ocean crust or continental crust with regard to rare earth element patterns and trace element concentrations or ratios, possibly implying multiple origins of zircons in jadeitite. Moreover, trace element data further suggest that ig-type Osayama zircons (and some Guatemalan zircons), unlike h-type zircons, are most likely to be of magmatic origin (see ESM S1.4).

Thirdly, the mineral inclusion assemblages in the h-type Osayama zircons are diagnostic; jadeite and rutile clearly link h-type zircons to the jadeitite-forming event. However, no mineral inclusions have been identified within ig-type Osayama zircons or Guatemalan zircons. Furthermore, mineral inclusions could form by replacement of other inclusions after zircon growth. At Syros, the presence of glaucophane and omphacite inclusions in some zircons from glaucophanite led Bröcker and Keasling (2006) to conclude that all the zircons from the Syros jadeitite and associated metasomatic reaction rinds formed during the Cretaceous HP metamorphism. Most zircons were examined in two dimensions (e.g., thin sections), and it may be that re-examination of these zircons by high-resolution CL imaging and/or confocal laser Raman microscope will distinguish between cognate mineral inclusions and minerals that grew along cracks or in cavities within zircon grains during the jadeitite-forming event.

Finally, zircon ages provide direct criteria for genesis, if the timing of magmatism and metamorphism in the region is well constrained. Although the U–Pb age ranges of h-type and ig-type zircons from the Osayama jadeitite overlap: 531 ± 38 (2 SE) to 447 ± 18 Ma, and 527 ± 20 to 488 ± 20 Ma (Tsujimori et al. 2005), the age range for the h-type zircons is much larger, extends to younger ages and they give a lower average age (~ 480 Ma) than ig-type zircons (~ 510 Ma). Furthermore, ig-type zircons occur as

cores in some h-type zircons (the reverse relation has not been observed) and are therefore demonstrably older than h-type zircons. If the calculated hafnium model age of the Osayama h-type zircons is geologically meaningful despite their complex history (magmatism, metasomatism, metamorphism and/or hydrothermal alteration), hafnium was remobilized from igneous protoliths of jadeitite and thus the model age may represent the timing of melt (ultimate source) differentiated from the mantle at ~ 570 Ma (Fig. 4). In this regard, the fluids responsible for formation of h-type zircons may have interacted extensively with serpentinized peridotites or mafic rocks in the same mélange. Elsewhere, the presence of two types of zircon in jadeitite is supported by a recent study employing in situ ion microprobe U–Pb dating. Shi et al. (2008) identified two generations of zircon in jadeitite from Myanmar: 163.2 ± 6.6 Ma (2 SE) for inherited zircons and 146.5 ± 6.8 Ma for hydrothermal zircons, with one younger outlier (122.2 ± 9.6 Ma). It is noted that $\varepsilon_{\text{Hf}}(t)$ values for all these Burmese zircons are very high, from +15.5 to +20.0, interpreted to be derived from rapid reworking of very juvenile crust (Shi et al. 2009).

The zircon U–Pb age (154 Ma) for the Guatemalan phengite jadeitite is older than published $^{40}\text{Ar}/^{39}\text{Ar}$ ages of phengitic mica in diverse HP rock types from the south side of the Motagua Fault Zone, Guatemala (125 to 113 Ma; Harlow et al. 2004) or Sm–Nd mineral isochron ages of eclogites from both sides of the Motagua Fault Zone (125 to 141 Ma; Martens et al. 2007; Brueckner et al. 2009). This age difference (~ 10 to 40 Ma) indicates that the zircons in the Guatemalan phengite jadeitite grew prior to the Cretaceous HP metamorphism. Chiari et al. (2006) reported radiolarian biostratigraphic evidence for a Late Jurassic age of the (Río) El Tambor Group ophiolites in Guatemala. The HP rocks are interpreted as an exhumed subduction-channel boundary zone from a Cretaceous collision of the Chortís block with the North American plate and exposed adjacent to the Motagua Fault (Harlow et al. 2004; Brueckner et al. 2009), although there are other tectonic interpretations (e.g., Donnelly et al. 1990; Beccaluva et al. 1995; Solari et al. 2009).

Summary and conclusions

Based on morphology, textures, mineral inclusions, and/or chemical and isotopic compositions, zircons in jadeitite can be classified into two groups: the first group (hydrothermal/metasomatic) corresponds to h-type zircons from the Osayama jadeitite and the second group (remnant igneous zircon from protoliths) includes ig-type zircons from the Osayama, many zircons from the Guatemalan phengite jadeitite and all examined zircons from the Syros jadeitite

(and associated metasomatic reaction rinds). We conclude that the ig-type Osayama zircons, many Guatemalan zircons and the Syros zircons are inherited from pre-existing igneous rocks, and that only the h-type Osayama zircons and some of the low $\delta^{18}\text{O}$ Guatemalan zircons are consistent with a hydrothermal origin. Although previous petrogenetic studies have emphasized the importance of direct precipitation from hydrothermal fluids, the results of this study suggest that metasomatic replacement and alteration of pre-existing igneous rocks is important. Thus, zircons in eclogite facies rocks may have a more prolonged and more interesting history than previously thought.

Acknowledgments B. Hess helped with sample preparation, B. Selleck (Colgate University) assisted with SEM-CL imaging of the zircons from Guatemala, and A. Greig and J. Woodhead assisted with laser ablation ICP-MS analysis. R. Maas, I.N. Bindeman, four anonymous referees and the journal editor J. Hoefs reviewed an earlier version of this manuscript. This work was partly supported by the National Science Foundation (EAR-0509639, 0838058), US Department of Energy (93ER14389), and the Japan Society for the Promotion of Science, Grant-in-Aid for Young Scientists (B) (13740312) and for Scientific Research (B) (21340148). The Wisc-SIMS Laboratory is partially supported by the National Science Foundation (EAR-0319230, EAR-0516725, EAR-0744079).

References

- Beccaluva L, Bellia S, Coltorti M, Dengo G, Giunta G, Mendez J, Romero J, Rotolo S, Siena F (1995) The northwestern border of the Caribbean plate in Guatemala: new geological and petrological data on the Motagua ophiolitic belt. *Ofioliti* 20:1–15
- Black LP, Kamo SL, Allen CM, Aleinikoff JN, Davis DW, Korsch RJ, Foudoulis C (2003a) TEMORA 1: a new zircon standard for Phanerozoic U–Pb geochronology. *Chem Geol* 200:155–170
- Black LP, Kamo SL, Williams IS, Mundil R, Davis DW, Korsch RJ, Foudoulis C (2003b) The application of SHRIMP to Phanerozoic geochronology: a critical appraisal of four zircon standards. *Chem Geol* 200:171–188
- Black LP, Kamo SL, Allen CM, Davis DW, Aleinikoff JN, Valley JW, Mundil R, Campbell IH, Korsch RJ, Williams IS, Foudoulis C (2004) Improved $^{206}\text{Pb}/^{238}\text{U}$ microprobe geochronology by monitoring of a trace-element-related matrix effect: SHRIMP, ID-TIMS, ELA-ICP-MS and oxygen isotope documentation for a series of zircon standards. *Chem Geol* 205:115–140
- Bröcker M, Keasling A (2006) Ion probe U–Pb zircon ages from the high-pressure/low-temperature mélange of Syros, Greece: age diversity and the importance of pre-Eocene subduction. *J Metamorph Geol* 24:615–631
- Brueckner HK, Avé Lallemand HG, Sisson VB, Harlow GE, Hemming SR, Martens U, Tsujimori T, Sorensen SS (2009) Metamorphic reworking of a high pressure-low temperature mélange belt along the Motagua fault, Guatemala: a record of Neocomian and Maastrichtian transpressional tectonics. *Earth Planet Sci Lett* 284:228–235
- Cavosie AJ, Valley JW, Wilde SA, EIMF (2005) Magmatic $\delta^{18}\text{O}$ in 4400–3900 Ma detrital zircons: a record of the alteration and recycling of crust in the Early Archean. *Earth Planet Sci Lett* 235:663–681

- Cavosie AJ, Kita NT, Valley JW (2009) Magmatic zircons from the Mid-Atlantic Ridge: primitive oxygen isotope signature. *Am Mineral* 94:926–934
- Chiari M, Dumitrica P, Marroni M, Pandolfi L, Principi G (2006) Radiolarian biostratigraphic evidence for a Late Jurassic age of the El Tambor Group ophiolites (Guatemala). *Ophioliti* 31:141–150
- Coleman RG (1961) Jadeite deposits of the Clear Creek area, New Idria district, San Benito County, California. *J Petrol* 2:209–247
- Donnelly TW, Horne GS, Finch RC, López-Ramos E (1990) Northern Central America: the Maya and Chortís blocks. In: Dengo G, Case JE (eds) *The Caribbean region*, Geological Society of America, Boulder, pp 37–76
- Eiler JM (2001) Oxygen isotope variations of basaltic lavas and upper mantle rocks. In: Valley JW, Cole DR (eds) *Stable isotope geochemistry*, vol 43, *Rev Mineral Geochem*. Mineralogical Society of America/Geochemical Society, Washington, DC, pp 319–364
- Ferry JM, Watson EB (2007) New thermodynamic models and revised calibrations for the Ti-in-zircon and Zr-in-rutile thermometers. *Contrib Mineral Petrol* 154:429–437
- Fu B, Page FZ, Cavosie AJ, Clechenko CC, Fournelle J, Kita NT, Lackey JS, Wilde SA, Valley JW (2008) Ti-in-Zircon thermometry: applications and limitations. *Contrib Mineral Petrol* 156:197–215
- Grimes CB, John BE, Kelemen PB, Mazdab FK, Wooden JL, Cheadle MJ, Hanghøj K, Schwartz JJ (2007) Trace element chemistry of zircons from oceanic crust: a method for distinguishing detrital zircon provenance. *Geology* 35:643–646
- Grimes CB, John BE, Cheadle MJ, Mazdab FK, Wooden JL, Swapp S, Schwartz JJ (2009a) On the occurrence, trace element geochemistry, and crystallization history of zircon from in situ oceanic lithosphere. *Contrib Mineral Petrol*. doi:10.1007/s00410-009-0409-2
- Grimes C, Ushikubo T, John BE, Valley JW (2009b) Oxygen isotopic ratio of ocean zircon. *Geochim Cosmochim Acta* 73(13 Suppl 1): A466
- Harlow GE, Hemming SR, Avé Lallemand HG, Sisson VB, Sorensen SS (2004) Two high-pressure–low-temperature serpentinite-matrix mélange belts, Motagua fault zone, Guatemala: a record of Aptian and Maastrichtian collisions. *Geology* 31:17–20
- Harlow GE, Sorensen SS, Sisson VB, Jade (2007) In: Groat LA (ed) *The geology of gem deposits*, short course handbook series 37:207–253. Mineralogical Association of Canada, Quebec
- Hayasaka Y, Sugimoto T, Kano T (1995) Ophiolite complex and metamorphic rocks in the Niimi-Katsuyama area, Okayama Prefecture: excursion guidebook of 102nd annual meeting of the Geological Society of Japan, pp 71–87 (in Japanese)
- Hellstrom J, Paton C, Woodhead J, Hergt J (2008) Iolite: Software for spatially resolved LA-(QUAD and MC) ICPMS analysis. Mineralogical association of Canada short course series 40, pp 343–348, Mineralogical Association of Canada, Vancouver
- Johnson CA, Harlow GE (1999) Guatemala jadeitites and albitites were formed by deuterium-rich serpentinizing fluids deep within a subduction zone. *Geology* 27:629–632
- Katzir Y, Bröcker M, Valley JW, Spicuzza MJ (2002) Oxygen isotope variations in Cycladic eclogites: assessing the significance of zircon ages. *Geochim Cosmochim Acta* 66(15A):A386
- Kita NT, Ushikubo T, Fu B, Valley JW (2009) High precision SIMS oxygen isotope analyses and the effect of sample topography. *Chem Geol* 264:43–57
- Martens U, Solari L, Sisson V, Harlow G, Torres de León R, Ligorra JP, Tsujimori T, Ortega F, Brueckner H, Giunta G, Ave Lallemand H (2007) Field trip guide—first field workshop of IGCP 546 “subduction zones of the Caribbean”: high-pressure belts of central Guatemala: the Motagua suture and the Chuacús complex. 36 p. http://www.ugr.es/~agcasco/igcp546/Guate07/IGCP546_Guatemala2007_FieldTripGuide.pdf
- Matthews A, Goldsmith JR, Clayton RN (1983) Oxygen isotope fractionations involving pyroxenes: the calibration of mineral-pair thermometers. *Geochim Cosmochim Acta* 47:631–644
- Page FZ, Ushikubo T, Kita NT, Riciputi LR, Valley JW (2007a) High-precision oxygen isotope analysis of picogram samples reveals 2 μm gradients and slow diffusion in zircon. *Am Mineral* 92:1772–1775
- Page FZ, Fu B, Kita NT, Fournelle J, Spicuzza MJ, Schulze DJ, Viljoen F, Basei MAS, Valley JW (2007b) Zircons from kimberlite: new insights from oxygen isotopes, trace element, and Ti in zircon thermometry. *Geochim Cosmochim Acta* 71:3887–3903
- Paton C, Woodhead JD, Hergt JM, Hellstrom J, Greig A (2009) Improved laser ablation U–Pb geochronology through robust down-hole fractionation correction. *Geochem Geophys Geosyst* (in review)
- Putlitz B, Matthews A, Valley JW (2000) Oxygen and hydrogen isotope study of high-pressure metagabbros and metabasalts (Cyclades, Greece): implications for the subduction of oceanic crust. *Contrib Mineral Petrol* 138:114–126
- Shi GH, Cui WY, Cao SM, Jiang N, Jian P, Liu DY, Miao LC, Chu BB (2008) Ion microprobe zircon U–Pb age and geochemistry of the Myanmar jadeitite. *J Geol Soc London* 165:221–234
- Shi GH, Jiang N, Liu Y, Wang X, Zhang ZY, Xu YJ (2009) Zircon Hf isotope signature of the depleted mantle in the Myanmar jadeitite: implications for Mesozoic intra-oceanic subduction between the Eastern Indian Plate and the Burmese Platelet. *Lithos* 112:342–350
- Solari LA, Ortega-Gutiérrez F, Elías-Herrera M, Schaaf P, Norman M, Torres de León R, Ortega-Obregón C, Chiquín M, Morán-Ical S (2009) U–Pb zircon geochronology of Paleozoic units in Western and Central Guatemala: insights into the tectonic evolution of Middle America. In: James KH, Lorente MA, Pindell JL (eds) *The origin and evolution of the Caribbean plate*, vol 328. Geological Society of London, Special Publication, pp 293–311
- Sorensen SS, Harlow GE, Rumble D III (2006) The origin of jadeitite-forming subduction-zone fluids: CL-guided SIMS oxygen isotope and trace element evidence. *Am Mineral* 91:979–996
- Spicuzza MJ, Valley JW, McConnell VS (1998) Oxygen isotope analysis of whole rock via laser fluorination: an air-lock approach. *Geol Soc Am Abstr Prog* 30:80
- Stacey JS, Kramers JD (1975) Approximation of terrestrial lead isotope evolution by a two-stage model. *Earth Planet Sci Lett* 26:207–221
- Tomaschek F, Kennedy AK, Villa IM, Lagos M, Ballhaus C (2003) Zircons from Syros, Cyclades, Greece—Recrystallization and mobilization of zircon during high-pressure metamorphism. *J Petrol* 44:1977–2002
- Tsujimori T, Liou JG, Wooden J, Miyamoto T (2005) U–Pb dating of large zircons in low-temperature jadeitite from the Osayama serpentinite mélange, SW Japan: insights into the timing of serpentinization. *Int Geol Rev* 47:1048–1057
- Tsujimori T, Liou JG, Coleman RG (2007) Finding of high-grade tectonic blocks from the New Idria serpentinite body, Diablo Range, California: petrologic constraints on the tectonic evolution of an active serpentinite diapir. In: Cloos M, Carlson WD, Gilbert MC, Liou JG, Sorensen SS (eds) *Convergent margin terranes and associated regions: a tribute to W.G. Ernst*. *Geol Soc Am Spec Paper* 419:67–80. Geological Society of America, Denver
- Valley JW (2001) Stable isotope thermometry at high temperatures. In: Valley JW, Cole DR (eds) *Stable isotope geochemistry*, vol 43, *Rev Mineral Geochem*. Mineralogical Society of America/Geochemical Society, Washington, DC, pp 365–413

- Valley JW (2003) Oxygen isotopes in zircon. In: Hanchar JM, Hoskin PWO (eds) *Zircon*, vol 53, *Rev Mineral Geochem*. Mineralogical Society of America/Geochemical Society, Washington, DC, pp 343–385
- Valley JW, Kita NT (2009) In situ oxygen isotope geochemistry by ion microprobe. In: Fayek M (ed) *MAC Short Course: secondary ion mass spectrometry in the earth sciences*, vol 41, pp 19–63
- Valley JW, Kitchen N, Kohn MJ, Niendorf CR, Spicuzza MJ (1995) UWG-2, a garnet standard for oxygen isotope ratios: strategies for high precision and accuracy with laser heating. *Geochim Cosmochim Acta* 59:5223–5231
- Valley JW, Bindeman IN, Peck WH (2003) Empirical calibration of oxygen isotope fractionation in zircon. *Geochim Cosmochim Acta* 67:3257–3266
- Valley JW, Lackey JS, Cavosie AJ, Clechenko CC, Spicuzza MJ, Basei MAS, Bindeman IN, Ferreira VP, Sial AN, King EM, Peck WH, Sinha AK, Wei CS (2005) 4.4 billion years of crustal maturation: oxygen isotopes in magmatic zircon. *Contrib Mineral Petrol* 150:561–580
- Watson EB, Wark DA, Thomas JB (2006) Crystallization thermometers for zircon and rutile. *Contrib Mineral Petrol* 151:413–433
- Wiedenbeck M, Alle P, Corfu F, Griffin WL, Meier M, Oberli F, Von Quadt A, Roddick JC, Spiegel W (1995) Three natural zircon standards for U-Th-Pb, Lu-Hf, trace element and REE analyses. *Geostand News* 19:1–23
- Woodhead J, Hergt J, Shelley M, Eggins S, Kemp R (2004) Zircon Hf-isotope analysis with an excimer laser, depth profiling, ablation of complex geometries, and concomitant age estimation. *Chem Geol* 209:121–135

ELECTRONIC SUPPLEMENTARY MATERIAL S1

S1.1 SAMPLE DESCRIPTIONS AND GEOCHRONOLOGY

OSAYAMA, SW JAPAN

Two jadeitite samples (OSJ-A & B) were collected from an outcrop of weathered jadeitite veins associated with blueschist, omphacite, albitite and rodingite in the Osayama serpentinite mélange, SW Japan (e.g., Tsujimori et al. 2005). Zircons up to 3mm in size were handpicked from this outcrop. Jadeitite samples are nearly monomineralic jadeite, and contain trace grossular-rich garnet, rutile and zircon. Rutile inclusions are found in both jadeite and zircon (Tsujimori et al. 2005). Retrograde minerals include omphacite, titanite, pectolite, and analcime. Coarse-grained rutile (up to 4 mm long) occurs in the jadeite-dominant matrix and is rimmed by secondary titanite that is in contact with pectolite (Tsujimori et al. 2005). P-T conditions of jadeitite, based on phase equilibria, are > 12 kbar and < 350°C (Tsujimori et al. 2005). Eight crystals of zircon were dated by in-situ U-Pb ion microprobe (SHRIMP-RG) techniques (Tsujimori et al. 2005). The $^{206}\text{Pb}/^{238}\text{U}$ age of the zircons varies from 523 to 454 Ma, in agreement with thermal ionization mass spectrometer (TIMS) U-Pb zircon ages of ~500 to 450 Ma (Miyamoto and Yanagi 1999). Gabbro dikes within serpentinitized peridotites (mainly harzburgite) yield a Sm-Nd isochron (whole-rock–mineral) age of ~560 Ma (Hayasaka et al. 1995). This suggests a Cambrian ophiolite sequence. Phengite K-Ar ages of blueschist-facies schists from the Osayama serpentinite mélange range between 327 and 273 Ma, which is thought to represent regional Late Paleozoic blueschist-facies metamorphism (Tsujimori and Itaya 1999).

SYROS, GREECE

A suite of mélange samples was studied from Syros, Greece: jadeitite (sample 3148), and associated omphacitite (3149), glaucophanite (3150), and chlorite-actinolite schist (3152) (Bröcker and Keasling 2006). Jadeitite mostly consists of jadeite and albite in the absence of quartz or rutile.

Titanite, allanite, zircon, white mica, chlorite, and apatite occur as trace minerals. Omphacitite consists of omphacite (55 vol. %), albite (25%), white mica (5%), titanite, zircon, chlorite, and opaque minerals. Glaucophanite consists mostly of glaucophane with minor omphacite, rutile, titanite, zircon, allanite, white mica, and biotite. Sample 3152 consists of chlorite (60%), actinolite (30%), rutile, zircon, talc, and apatite. The HP metamorphic conditions in this region were 450° to 550°C and 12 to 20 kbar (e.g., Ridley 1984; Trotet et al. 2001; Katzir et al. 2007; Chalmers et al. 2007). In all four samples, zircon displays a euhedral short-prismatic or blocky morphology and may contain rutile inclusions except for jadeitite (3148). Glaucophane and omphacite inclusions in zircons from the glaucophanite have also been reported (Bröcker and Enders 1999; Bröcker and Keasling 2006). As illustrated by Bröcker and Keasling (2006), there are also some elongated prismatic zircon grains, notably in the smaller grain size fractions (< 125 µm), for glaucophanite (3150) and chlorite-actinolite rinds (3152). Cathodoluminescence (CL) patterns of zircon commonly show regular oscillatory or sector zoning, or homogenous featureless domains. Some grains reveal complex, disturbed internal CL structures (see Figures 7c & f of Bröcker and Keasling 2006) that are related to solid-state recrystallization caused by unmixing of trace elements from the crystal lattice (Bröcker and Enders 1999).

Zircons from Syros have a variable U and Th content: from 8 to 737 ppm U and 2 to 1096 ppm Th. The Th/U ratio ranges between 0.29 and 1.54. Zircons from this suite of mélange samples as well as from a vein-fractured metabasic host rock (M. Bröcker, unpublished data) yielded $^{206}\text{Pb}/^{238}\text{U}$ ages of 79.6 to 79.8 Ma, in reasonable agreement with igneous zircons from plagiogranite occurring in other mélange blocks (e.g., $76.6 \pm 1.3\text{Ma}$; Bröcker and Keasling 2006).

The timing of high-pressure metamorphism for the Syros mélange and, at a broader scale, the Cyclades, Greece, is controversial. It is unclear if there were one or two stages of HP metamorphism (~80 and 52 Ma, *versus* 52 Ma only). The ~80 Ma zircons in jadeitite are important evidence in this debate. If hydrothermal, they would suggest HP metamorphism at this time, but it is also possible that they are inherited from known magmatic rocks of this age.

GUATEMALA

Two samples of jadeitite were studied from Guatemala. Sample MVE02-8-6 is a phengite jadeitite from Quebrada El Silencio, close to the town of Carrizal Grande, Guatemala. It came from a block associated with lawsonite eclogite in serpentinite matrix mélangé within the Chortís block from the south side of the Motagua Fault. Compared with other serpentinite mélanges (e.g., Franciscan in California, Cordillera de la Costa in Venezuela, Samaná peninsula in Dominican Republic), this one is dominated by massive antigorite serpentinite with HP-LT blocks along interior faults, and only minor metasediments. The jadeitite consists of phengitic muscovite, jadeite, and omphacite with minor quartz, titanite, rutile, zircon, allanite, monazite and secondary albite. Rutile, zircon and monazite are typically found either as small grains in cores of titanite, or as larger grains in jadeite and phengite, and along grain boundaries. Zircons are generally small, < 100 µm long, euhedral, and contain rare, so-far unidentified inclusions. They commonly occur as inclusions in jadeite and phengite and display rhythmic zoning. Phengitic micas from the HP-LT rocks give a $^{40}\text{Ar}/^{39}\text{Ar}$ age ranging from 125 to 113 Ma (Harlow et al. 2004). A Sm-Nd mineral isochron for eclogites from the south side of the Motagua Fault gives an age of 131.7 ± 6.7 (2 standard errors, SE) and 140.6 ± 3.4 Ma (Martens et al. 2007; Brueckner et al. 2009).

Sample MVE02-39-6 is a jadeitite from a boulder field called Pica Pica along the Atlantic Highway between Ríos Uyus and Uijó north of the Motagua Fault zone within the Maya block (Harlow 1994; Giunta et al. 2002; Martens et al. 2007). It contains jadeite, omphacite, phlogopite, phengite, albite, analcime, titanite, rutile, and zircon. Titanite can have cores of rutile or zircon, and only zircon occurs as inclusions in jadeite and along grain boundaries. Zircons are small, < 100 µm across, and inclusions in them have not been observed. $^{40}\text{Ar}/^{39}\text{Ar}$ measurements on white micas yield an age of 65 to 77 Ma (Harlow et al. 2004). Sm-Nd mineral isochrons of eclogites from the north side of the Motagua Fault give ages of 125.0 ± 7.8 (2 SE) and 130.7 ± 6.3 Ma (Martens et al. 2007).

NEW IDRIA, CALIFORNIA

New Idria is a classic locality of jadeitite from Franciscan Complex in California, where Coleman (1961) first described centimeter-scale jadeitite veins cutting blueschist. Tsujimori et al. (2007) reported the presence of high-grade tectonic blocks including jadeite-bearing retrograded

eclogite, pumpellyite-rich retrograded eclogite, and clinopyroxene-bearing garnet-amphibolite in the jadeitite-bearing New Idria serpentinite body. The New Idria serpentinite body consists mainly of chrysotile-lizardite serpentinite and minor antigorite serpentinite. Therefore, the New Idria serpentinite diapir is thought to be derived from mantle depths that incorporated tectonic blocks at various mantle-crustal levels during exhumation (Tsujimori et al. 2007). The samples investigated in this study include: an early jadeitite vein (> 97% jadeite by modal volume, sample NIJ-Jd); a late pure albite vein (NIJ-Ab); and a blueschist host-rock (NIJ-Host) of the crosscutting jadeitite vein. The presence of retrograde jadeite and lawsonite in eclogite within serpentinite from New Idria indicates blueschist-facies overprinting ($P > 10$ kbar at $T \sim 250^\circ$ to 300°C) subsequent to eclogite-facies metamorphism, and these jadeitites probably formed at the same conditions (Tsujimori et al. 2007).

S1.2 ANALYTICAL METHODS

Both secondary electron and CL imaging of standard zircons (KIM-5) and unknown zircons from the Guatemala phengite jadeitite (Fig. S1.1) were conducted using a JSM-6360LV scanning electron microscope with a Centaurus CL detector at Colgate University (15 kV accelerating voltage, 21 mm working distance).

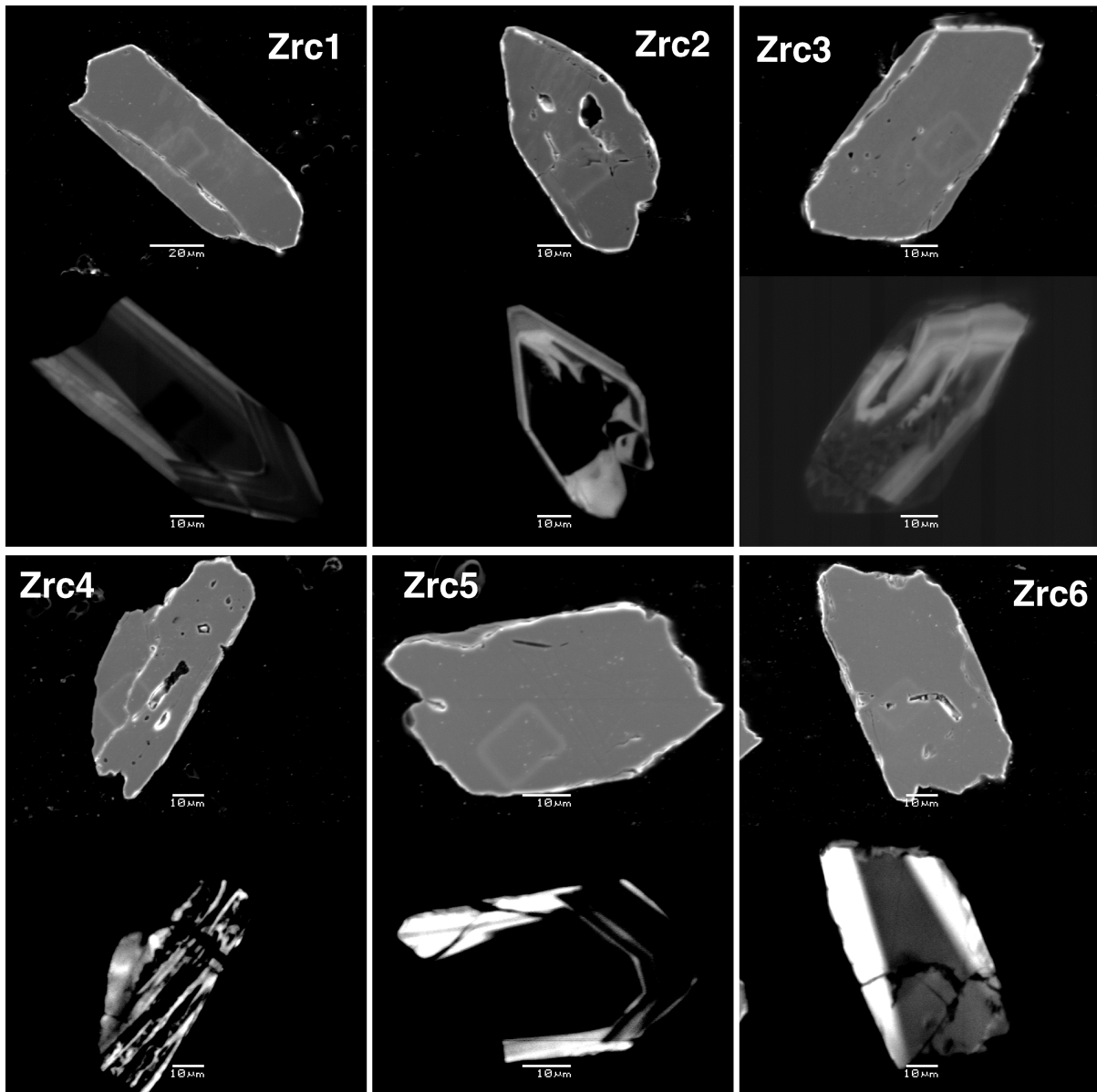


Figure S1.1 Secondary electron and cathodoluminescence images of zircons (Zrc1 to Zrc6) from the Guatemalan phengite jadeite by Scanning electron microscope.

Bulk oxygen isotope analyses of whole-rock or jadeite powders were performed at the University of Wisconsin – Madison, by laser fluorination as described by Valley et al. (1995) and Spicuzza et al. (1998). Oxygen isotope ratios ($^{18}\text{O}/^{16}\text{O}$) were measured on a gas source Finnigan MAT 251 mass spectrometer, and are reported in standard δ -notation relative to Vienna Standard Mean Ocean Water (VSMOW). All $\delta^{18}\text{O}$ values were corrected to the VSMOW scale using the UWG-2 Gore Mountain garnet standard ($\delta^{18}\text{O} = 5.80\text{‰}$; Valley et al. 1995).

Ion microprobe analyses of $^{18}\text{O}/^{16}\text{O}$ ratios and trace element (Ti & REEs, or rare earth elements) concentrations in zircons were made on a CAMECA IMS-1280 ion microprobe at the University of Wisconsin – Madison. The working conditions and data reduction are described in detail elsewhere (Page et al. 2007a, b; Kita et al. 2009; Valley and Kita 2009) and are not repeated here. The locations of ion microprobe analysis spots for oxygen isotopes, Ti and/or REE concentrations were correlated, if applicable, with the SHRIMP U-Pb pits for the Osayama and Syros zircons, while the Guatemalan zircons were thereafter dated by laser ablation ICP-MS (inductively coupled plasma mass spectrometer).

Hf isotopes. Hafnium isotope data for Osayama zircons, obtained using a 55 μm diameter ablation spot, were measured on a Nu Plasma multi-collector ICP-MS as described by Woodhead et al. (2004). Isotopic drift was monitored against $^{176}\text{Hf}/^{177}\text{Hf} = 0.281630$ for the BR-266 zircon. Reproducibility was assessed through frequent analysis of Temora zircon: nine analyses performed throughout the analytical session averaged 0.282700 ± 23 (2 SE, total range 0.282642-0.282737), in good agreement with a previously published value of 0.282686 (Woodhead et al. 2004). Two analyses of KIM-5 zircon averaged 0.282660 ± 24 (2 SE), or $\epsilon_{\text{Hf}}(t=92 \text{ Ma}) = +2.1$; no reference Hf isotope data are available for this zircon. All the data are listed in Electronic supplementary materials (ESM) S5.

U-Pb. Laser ablation U-Pb and hafnium isotope analyses were carried out after all the SIMS analyses above at the University of Melbourne, using the 193 nm excimer laser-based HELEX ablation system described in Woodhead et al. (2004). The zircon grain mounts were cleaned after removal of coated gold. For U-Pb geochronology of zircons with oscillatory zoning (Fig. S1.1) from the Guatemalan jadeitites, a 32 μm spot size was used and U-Th-Pb isotopic abundances were measured in a Varian quadrupole ICP-MS, with the 91500 zircon (Wiedenbeck et al. 1995) as a primary standard. All data manipulation was done offline using the locally developed Iolite software package (Hellstrom et al. 2008) using the U-Pb data reduction module of Paton et al. (2009). The results obtained for the standard zircons Temora ($416.3 \pm 4.9 \text{ Ma}$, 2 SD, $n=4$) and KIM-5 ($92.1 \pm 2.8 \text{ Ma}$, $n=3$) obtained are consistent with previously published ages (Temora $416.8 \pm 2.6 \text{ Ma}$, isotope dilution thermal ionization mass spectrometer or ID-TIMS, Black et al. 2003a,b, 2004; KIM-5 92 ± 3

Ma, SIMS, Cavosie et al. 2005). The decay constants employed for U and Th are: $\lambda^{238}\text{U} = 0.155125 \times 10^{-9}/\text{yr}$, $\lambda^{235}\text{U} = 0.98485 \times 10^{-9}/\text{yr}$, and $\lambda^{232}\text{Th} = 0.049475 \times 10^{-9}/\text{yr}$.

S1.3 ZIRCON CRYSTALLIZATION TEMPERATURE

Zircon commonly crystallizes at high temperatures in magmatic or high-grade metamorphic rocks. However, low temperature (< 450°C) formation of zircon has also been proposed in diverse geological environments, including: intrusion-associated hydrothermal alteration or Au-REE mineralization (e.g., Hoskin and Schaltegger 2003 and references therein; Pettke et al. 2005; Hoskin 2005; Kebede et al. 2007; Pelletier et al. 2007) and low-grade metamorphism or serpentization (e.g., Dubinska et al., 2004; Dempster et al. 2004; Rasmussen 2005). Therefore, the Ti-in-zircon thermometer, if extrapolated to lower temperatures than recommended and applied with idealized simplifying assumptions, theoretically can be used to distinguish low-temperature, hydrothermal zircons from high-temperature, magmatic (or high-grade metamorphic) zircons.

Using the calibration of Watson and Harrison (2005) and Watson et al. (2006) with no correction for reduced activity or pressure, apparent Ti-in-zircon temperatures estimated for the Osayama zircons vary between 571° and 720°C (average: $647 \pm 85^\circ\text{C}$) (ESM S3 & S4). The average apparent Ti-in-zircon temperatures are: $617 \pm 53^\circ\text{C}$ (2 SD, n=16), for ig-type zircons; and $677 \pm 67^\circ\text{C}$ (n=16), for h-type zircons. At Syros, the apparent Ti-in-zircon temperatures average $733 \pm 51^\circ\text{C}$ (2 SD, n=22; 669° to 773°C) for jadeitite, and $721 \pm 70^\circ\text{C}$ (n=42; 652° to 785°C) for associated rocks. For the Guatemalan zircons, apparent Ti-in-zircon temperatures average $759 \pm 80^\circ\text{C}$ (2 SD, n=11), varying from 676° to 803°C.

The apparent uncorrected Ti-in-zircon temperatures determined for the zircons studied here, as well as the presumed hydrothermal zircons from a metasomatic rodingite shell of Sudetic ophiolite, SW Poland ($683 \pm 20^\circ\text{C}$; M. Bröcker, unpublished data; cf. Dubinska et al. 2004), are comparable to those for the majority of igneous zircons in mafic to felsic rocks (~600° to 850°C; Watson et al. 2006; Fu et al. 2008), but they all exceed the likely maximum temperatures for their host rocks (jadeitites) (mostly $\leq 450^\circ\text{C}$; up to 550°C for Syros; Trotet et al. 2001), as based on fluid inclusions, stable isotopes and thermobarometry (Harlow et al. 2007 and references therein). This inconsistency

suggests that either those estimates based on Ti-in-zircon thermometry are too high, or zircons are inherited from a pre-jadeitite higher-temperature stage, i.e., formed at or close to magmatic temperatures.

The main problem with the use of Ti-in-zircon temperatures for zircons of hydrothermal origin is the large potential departure from the basic assumptions of the thermometer for hydrothermal conditions. The critical parameter here is the silica activity. As long as zircons have equilibrated, and activities of TiO_2 and SiO_2 and the effect of pressure during zircon formation can be estimated accurately, the Ti-in-zircon thermometer (Watson and Harrison 2005, Watson et al. 2006) is interpreted to be applicable to a wide range of rock types (Ferry and Watson 2007; Page et al. 2007b), although other factors such as subsolidus resetting of Ti compositions, non-Henry's Law substitution of Ti in zircon, disequilibrium crystallization from melts, or growth of zircons in late melts with evolved hydrous composition may practically limit its application as argued by Fu et al. (2008) and Hofmann et al. (2009). The most recent calibration of this thermometer (580°-1400°C, $P \approx 10$ kbar; Ferry and Watson 2007) is given as:

$$\log(\text{ppm, Ti-in-zircon}) = (5.711 \pm 0.072) - (4800 \pm 86)/T(\text{K}) - \log a_{\text{SiO}_2} + \log a_{\text{TiO}_2} \quad \text{Eqn (1)}$$

with a pressure correction of 5°C/kbar. For SiO_2 and TiO_2 activities typical of most silicic magmas ($a_{\text{SiO}_2} \geq 0.3$, 600° to 1200°C, Carmichael et al. 1970; $a_{\text{TiO}_2} \geq 0.6$, Watson and Harrison 2005; Watson et al. 2006; Hayden and Watson 2007), Ti-in-zircon temperatures would range from 594°C ($a_{\text{SiO}_2} = 0.3$, $a_{\text{TiO}_2} = 1$) to 729°C ($a_{\text{SiO}_2} = 1$, $a_{\text{TiO}_2} = 0.6$) at a typical zircon Ti content of 5 ppm at $P = 10$ kbar.

To the extreme, if silica activity is very low, $a_{\text{SiO}_2} = 0.151$, 0.024 or 0.002, h-type zircons like jadeite may crystallize at $T = 550^\circ\text{C}$, 450°C or 350°C , by extrapolation of the Ti-in-zircon thermometer, Eqn (1), to lower temperatures ($< 580^\circ\text{C}$). Here, $\text{Ti} = 5$ ppm, the average for h-type Osayama zircons, and $a_{\text{TiO}_2} = 1$, because rutile is present in the Osayama jadeitite. Such low a_{SiO_2} appears feasible during jadeitite formation because jadeitites are commonly in direct contact to serpentinites. Further studies are required.

S1.4 PROVENANCE DISCRIMINANT DIAGRAMS

Chondrite-normalized REE patterns for the Osayama zircons show the low La/Lu ratios, strong Ce enrichment and smooth Pr-Lu slopes characteristic of most zircons, regardless of origin (Hoskin 2005). In detail, considerable variation exists in inter-REE ratios for both ig-type and h-type of zircons. Light rare earth elements in h-type zircons appear to be less fractionated (Sm/La_N 4-20) than in ig-type (86-144) while MREE-HREE fractionations show similarly wide ranges in the two morphological types (Yb/Sm_N 63-152 and 61-196; ESM S4). Cerium excess is stronger in ig-type than h-type zircons (Ce/Ce^* 6-46 *versus* 62-77). Europium is particularly interesting: while five of the six analyses have Eu depletion (Eu/Eu^* 0.63-0.76; ESM S4) similar to average upper continental crust (0.72; Rudnick and Gao 2004), one ig-type zircon has Eu/Eu^* of 1.30, representing a rare example of a Eu-enriched zircon. The latter is identical to average lower continental crust (1.14; Rudnick and Gao 2004).

Trace elements in zircons have been used as petrological or tectonic discriminants (e.g., hydrothermal *versus* magmatic, oceanic crust *versus* continental crust), although the reliability of this approach has been disputed. Hoskin and Ireland (2000) compared REE patterns for zircons from various types of crustal igneous rocks from diverse tectonic environments as well as kimberlite, carbonatite and high-grade metamorphic rocks. While no trace element data are available for the Syros zircons which are not discussed here, our results indicate that zircons from the Guatemalan phengite jadeitite and ig-type zircons from the Osayama jadeitite hosted by serpentinite are indistinguishable from those in gabbro dikes from Mid-Atlantic Ridge near the Kane Transform with regards to oxygen isotope compositions (5.3 ± 0.8 , $n=68$, Cavosie et al. 2009) and REE distribution patterns (Fig. S1.2). All of these zircons from Osayama and Guatemala have $\delta^{18}\text{O}$ values similar to zircons in equilibrium with primitive magmas from the mantle (zircon $\delta^{18}\text{O} = 5.3 \pm 0.6\text{‰}$; Valley 2003). The REE distribution patterns of zircon from Guatemala and Osayama (ig-type) are also similar to typical igneous zircons from Manila plagiogranite (as well as from Syros ophiolite; Hoskin and Ireland 2000), but distinctive from the other zircons shown in Figure S1.2b including: metamorphic zircons coexisting with garnet in HP veins (Rubatto and Hermann 2003), high-grade metapelites (Whitehouse and Platt 2003) or mantle megacrysts (e.g., KIM-5; see also Page et al.

2007b), which have HREE distribution patterns that are relatively flat or have a slight negative slope. Crystallization of coexisting garnet that is commonly enriched in HREE can produce depletion in HREE in a rock, especially at subsolidus conditions in a closed system (Rubatto 2002). This is supported by new experiments of Rubatto and Hermann (2007), which indicate that the HREE partitioning between zircon and garnet (distribution coefficients, $D^{Zrc/Grt} > 1$) decreases with increasing temperature at $P = 20$ kbar. We recognize that, even if both zircon and garnet are present in jadeitite (i.e., Osayama), the two may not have formed at the same period of time. Harley and Kelly (2007) demonstrated that the chemical response of zircon in essentially dry igneous rocks to late granulite facies metamorphic overprinting may be weak or negligible and that Y and REE distribution data for metamorphic zircon and garnet may be away from equilibrium. It is noted that the Osayama zircons (ig-type and h-type) have ≤ 785 ppm Y (or ≤ 0.1 wt.% Y_2O_3), while at absence of garnet, the Guatemalan zircons contain Y of ≥ 4685 ppm (or ≥ 0.6 wt.% Y_2O_3) (ESM S4). Such high-Y values are reported for zircons from anorogenic tholeiitic plagiogranites, whilst zircon in orogenic granitoids is commonly Y-poor ($Y_2O_3 < 0.1$ wt.%; Pupin 2000).

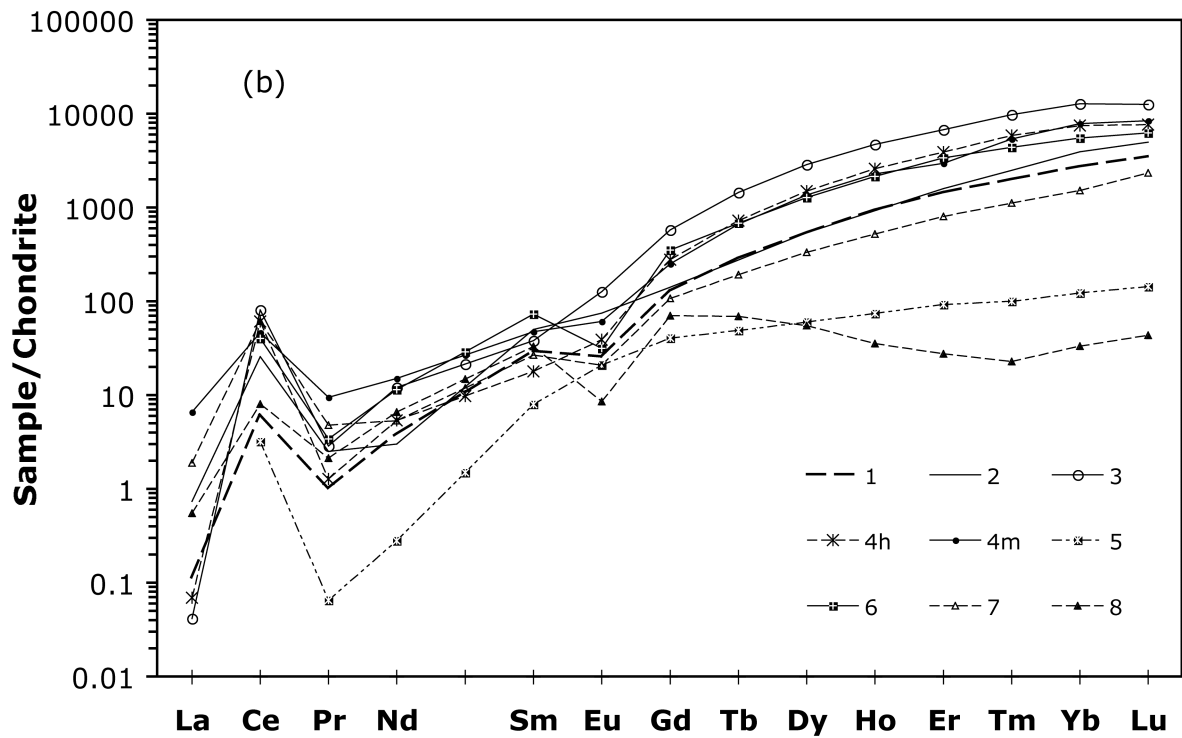
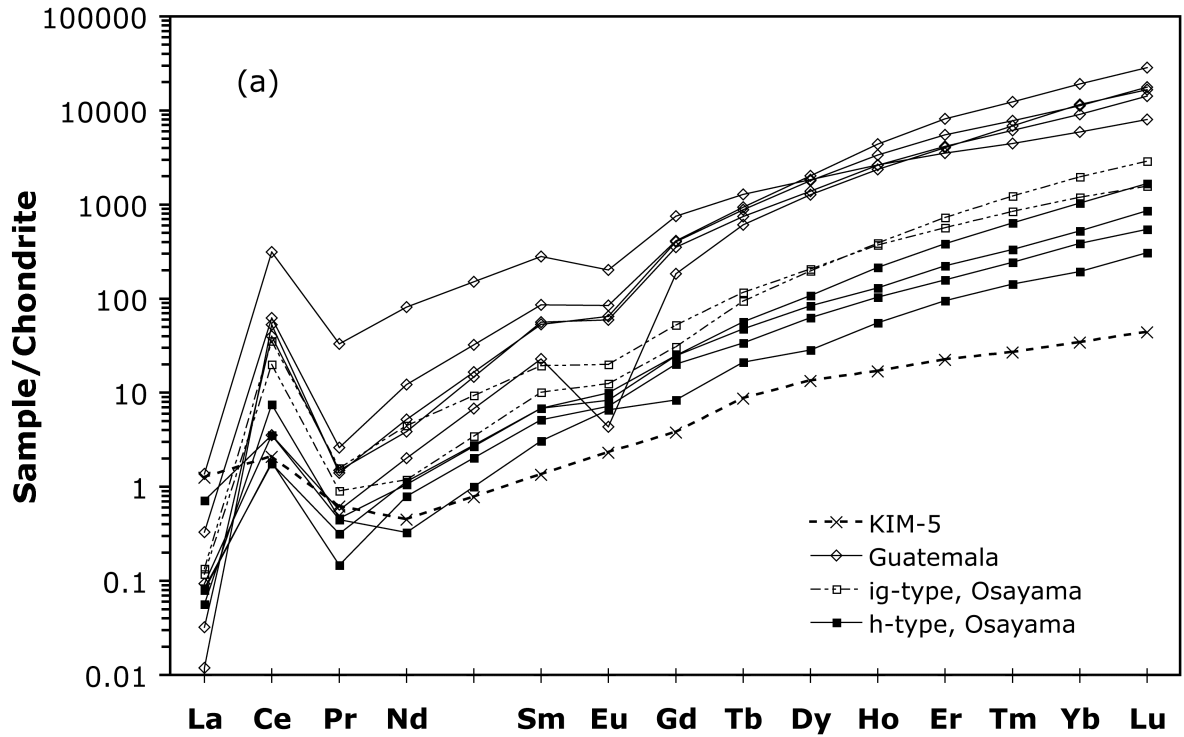


Figure S1.2 (a) REE distribution pattern of zircon in jadeitite from Osayama (ig-type and h-type), SW Japan and zircons in the Guatemalan phengite jadeitite, and zircon megacryst (KIM-5) from kimberlite. Normalized to C1 chondrite (McDonough and Sun 1995). Zircons in (1) ODP gabbros from Mid-Atlantic Ocean Ridge near the Kane Transform (Cavosie et al. 2009); (2) Manila plagiogranite (Hoskin and Ireland 2000); (3 to 4) igneous and hydrothermal or metamorphic (4h, 4m) zircons, Lugros eclogites

within the ophiolitic unit of the Mulhacén complex of the Betic Cordilleras in SE Spain (Puga et al. 2005); (5 & 6) eclogites and HP veins from Alps (Rubatto and Hermann 2003); (7 & 8) (*core and rim*) granulite-facies metapelites from the Betic Cordilleras in SE Spain (Whitehouse and Platt 2003) are also shown in (b), all on average, for comparison.

Grimes et al. (2007) proposed discriminant diagrams to distinguish igneous zircons from different geological settings (continental crust *versus* modern oceanic crust). In the present case, the Guatemalan zircons plot predominately in the U/Yb *versus* Hf (ppm) and U/Yb *versus* Y (ppm) fields of igneous zircons from modern ocean crust, and both types of zircon from the Osayama jadeitite (ig-type and h-type) in the fields of igneous zircons from continental crust (Figs. S1.3a & b; Grimes et al. 2007). This suggests that some of the zircons in jadeitite formed in ocean floor environments, while others may be relics of continentally derived sediment, subducted prior to the collisions that emplaced the subduction channel *mélange*.

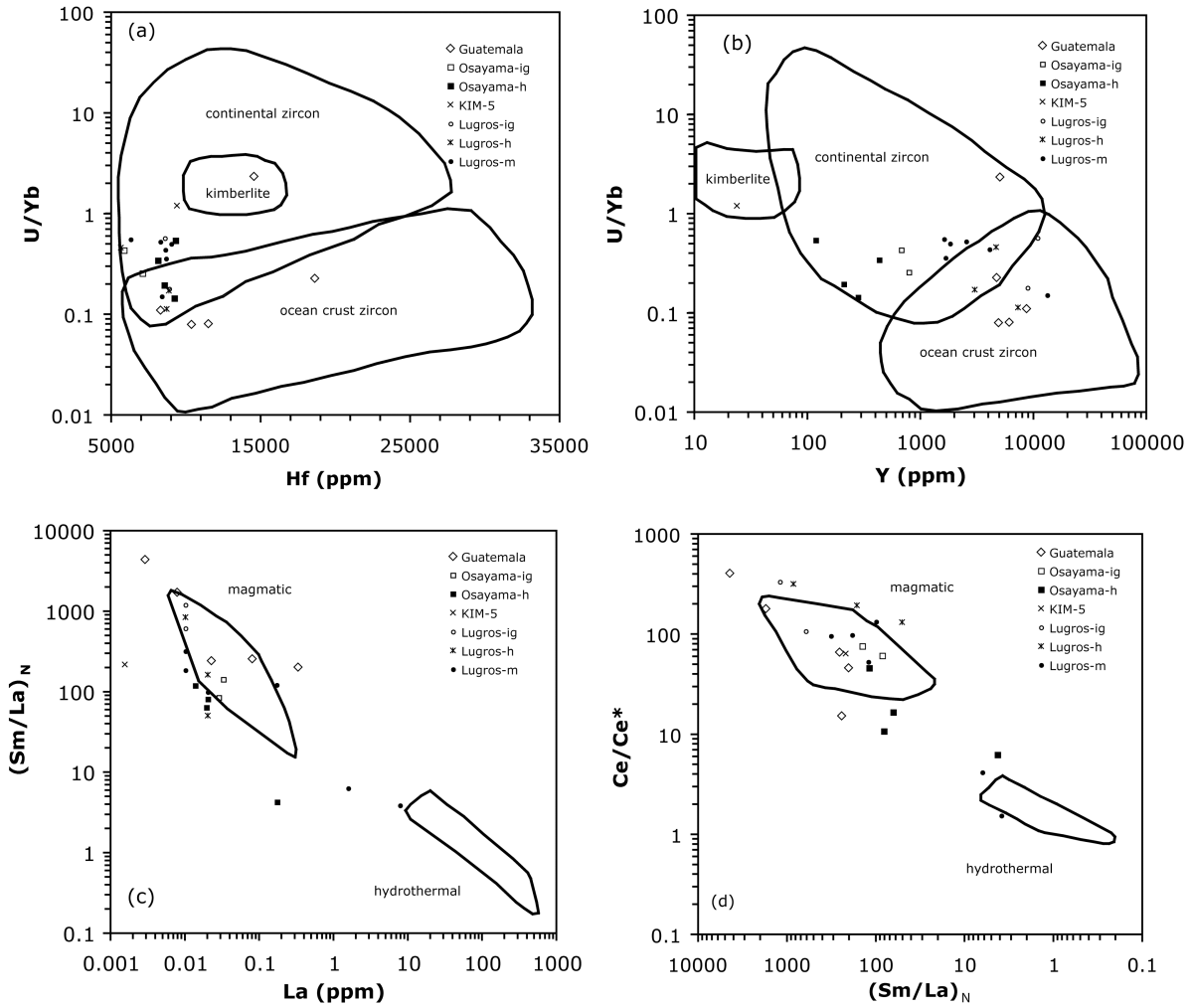


Figure S1.3 Discriminant diagrams of (a) U/Yb v. Hf (ppm), (b) U/Yb versus Y (ppm), (c) $(Sm/La)_N$ versus La (ppm), and (d) Ce/Ce* versus $(Sm/La)_N$, for zircons from the Osayama jadeitite (SW Japan) and the Guatemalan phengite jadeitite. Three areas in (a) and (b) are defined by zircons from kimberlite, continental crust and modern ocean crust (Grimes et al. 2007), and two areas in (c) and (d) are defined by magmatic and hydrothermal zircons from the Boggy Plain Zoned Pluton (Hoskin 2005). $(Sm/La)_N = (Sm/0.148)/(La/0.237)$, $Ce/Ce^* = (Ce/0.613)/\sqrt{(La/0.237)*(Pr/0.0928)}$; all chondrite values are taken from McDonough and Sun (1995). Data sources: (1) Zircons (Lugros-ig, h, m: igneous, hydrothermal, metamorphic) in the Lugros eclogites within the ophiolitic unit of the Mulhacén complex of the Betic Cordilleras in SE Spain, Puga et al. (2005); (2) zircon megacryst from kimberlite, KIM-5, ig-type and h-type zircons in the Osayama jadeitite, and zircons in the Guatemalan phengite jadeitite, this study.

Hoskin (2005) employed different discriminant diagrams to distinguish hydrothermal and magmatic zircons from the Boggy Plain Zoned Pluton aplite in the Lachlan Orogen, SE Australia. In

both $(\text{Sm}/\text{La})_N$ versus La (ppm) and Ce/Ce^* versus $(\text{Sm}/\text{La})_N$ plots as shown in Figs. S1.3c & d, most of the zircons in this study plot on or near the field defined by magmatic zircons from the Boggy Plain Zoned Pluton (Hoskin 2005). Only one h-type zircon from the Osayama jadeitite falls toward the field of hydrothermal zircons from the Boggy Plain Zoned Pluton aplite (Hoskin 2005; Figs. S1.3c & d). Here, we can only conclude that at least some h-type zircons, in contrast with ig-type zircons, from the Osayama jadeitite are most likely hydrothermal in origin.

Another example to distinguish hydrothermal and igneous zircons from ocean crust is also illustrated in Fig. S1.3 for zircons from Lugros eclogites within the ophiolitic unit of the Mulhacén complex of the Betic Cordilleras in SE Spain. The Lugros zircons are proposed to have formed at three different stages (Puga et al. 2005): a) crystallization of basaltic magma; b) high-temperature, seafloor alteration; and (c) HP metamorphism. The Th/U ratio for the zircons varies from 0.13 to 5.67 (Puga et al. 2005). As shown in Figs. S1.3c & d, only two data points for metamorphic zircons from the Lugros eclogites, none for hydrothermal zircons, fall near the field of hydrothermal zircons from the Boggy Plain Zoned Pluton aplite (Hoskin 2005). This indicates that, if the classification of magmatic and hydrothermal zircons from the Lugros eclogites (Puga et al. 2005) is correct, the discriminant diagrams proposed by Hoskin (2005) for hydrothermal and magmatic zircons from the Boggy Plain Zoned Pluton aplite may not be directly applicable to zircons from ocean crust. To sum up, the Guatemalan zircons may be inherited from ocean crust, whereas ig-type and h-type zircons from the Osayama jadeitite may have formed in continental crust, and h-type zircons are more likely to be hydrothermal than ig-type zircons.

REFERENCES (other than those listed in main text)

- Bröcker M, Enders M (1999) U-Pb zircon geochronology of unusual eclogite-facies rocks from Syros and Tinos (Cyclades, Greece). *Geol Mag* 136: 111–118
- Chalmers P, Spear FS, Cheney JT (2007) Zr-in-rutile thermometry in blueschists of Syros, Greece. *Geol Soc Am Abstr Prog* 39: 86
- Dempster TJ, Hay DC, Bluck BJ (2004) Zircon growth in slate. *Geology* 32: 221–224
- Dubinska E, Bylina P, Kozłowski A, Dörr W, Nejbort K, Schastok J, Kulicki C (2004) U-Pb dating of serpentinitization: hydrothermal zircon from a metasomatic rodingite shell (Sudetic ophiolite, SW Poland). *Chem Geol* 203: 183–203
- Giunta G, Beccaluva L, Coltorti M, Cutrupia D, Dengo C, Harlow GE, Mota B, Padoa E, Rosenfeld J, Siena F (2002) The Motagua Suture Zone in Guatemala. *Field Trip – Guide Book, IGCP 433 Workshop and 2nd Italian – Latin American Geological Meeting. Ofioliti* 27: 47–72

- Harley SL, Kelly NM (2007) The impact of zircon-garnet REE distribution data on the interpretation of zircon U-Pb ages in complex high-grade terrains: an example from Rauer Islands, East Antarctica. *Chem Geol* 241: 62–87
- Harlow GE (1994) Jadeitites, albitites, and related rocks from the Motagua Fault Zone, Guatemala. *J Metamorphic Geol* 12: 49–68
- Hayden LA, Watson EB (2007) Rutile saturation in hydrous siliceous melts and its bearing on Ti-thermometry of quartz and zircon. *Earth Planet Sci Lett* 258: 561–568
- Hofmann AE, Valley JW, Watson EB, Cavosie, AJ, Eiler JM (2009) Sub-micron scale distributions of trace elements in zircon. *Contrib Mineral Petrol* 158:317–335
- Hoskin PWO (2005) Trace-element composition of hydrothermal zircon and the alteration of Hadean zircon from the Jack Hills, Australia. *Geochim Cosmochim Acta* 69: 637–648
- Hoskin PWO, Ireland TR (2000) Rare earth element chemistry of zircon and its use as a provenance indicator. *Geology* 28: 627–630
- Hoskin PWO, Schaltegger U (2003) The composition of zircon and igneous and metamorphic petrogenesis. In: Hancher JM, Hoskin PWO (eds) *Zircon. Rev Mineral Geochem* 53: 27–62. Mineralogical Society of America/Geochemical Society, Washington, DC
- Katzir Y, Garfunkel Z, Avigad D, Matthews A (2007) The geodynamic evolution of the Alpine orogen in the Cyclades (Aegean Sea, Greece): insights from diverse origins and modes of emplacement of ultramafic rocks. In: Taymaz T, Yilmaz Y, Dilek Y (eds) *The Geodynamics of the Aegean and Anatolia*. *Geol Soc London Spec Publ* 291: 17–40
- Kebede T, Horie K, Hidaka H, Terada K (2007) Zircon ‘microvein’ in peralkaline granitic gneiss, western Ethiopia: origin, SHRIMP U–Pb geochronology and trace element investigations. *Chem Geol* 242: 76–102
- McDonough WF, Sun S-s (1995) The composition of the Earth. *Chem Geol* 120: 223–253
- Miyamoto T, Yanagi T (1999) U-Pb dating of zircon in jadeite rock in Osayama serpentinite mélange from Okayama Prefecture, Southwest Japan: 1999 Joint Annual Meeting of The Japanese Association of Mineralogists, Pathologists and Economic Geologists, and the Mineral Society of Japan, Abstr, pp 190 (in Japanese)
- Pelleter E, Cheilletz A, Gasquet D, Mouttaqi A, Annich M, El Hakour A, Deloule E, Féraude G (2007) Hydrothermal zircons: a tool for ion microprobe U–Pb dating of gold mineralization (Tamlalt–Menhouhou gold deposit — Morocco). *Chem Geol* 245: 135–161
- Pettke T, Audétat A, Schaltegger U, Heinrich CA (2005) Magmatic-to-hydrothermal crystallization in the W-Sn mineralized Mole Granite (NSW, Australia). Part II: Evolving zircon and thorite trace element chemistry. *Chem Geol* 220: 191–213
- Puga E, Fanning CM, Nieto JM, Díaz de Federico A (2005) Recrystallization textures in zircon generated by ocean-floor and eclogite-facies metamorphism: a cathodoluminescence and U-Pb SHRIMP study, with constraints from REE elements. *Can Mineral* 43: 183–202
- Pupin JP (2000) Granite genesis related to geodynamics from Hf-Y in zircon. *Trans Roy Soc Edinb (Earth Sci)* 91: 245–256.
- Rasmussen B (2005) Zircon growth in very low grade metasedimentary rocks: evidence for zirconium mobility at ~250°C. *Contrib Mineral Petrol* 150: 146–155
- Ridley J (1984) Evidence of a temperature-dependent ‘blueschist’ to ‘eclogite’ transformation in high-pressure metamorphism of metabasic rocks. *J Petrol* 25: 852–870
- Rubatto D (2002) Zircon trace element geochemistry: partitioning with garnet and the link between U-Pb ages and metamorphism. *Chem Geol* 184: 123–138
- Rubatto D, Hermann J (2003) Zircon formation during fluid circulation in eclogites (Monviso, Western Alps): implications for Zr and Hf budget in subduction zones. *Geochim Cosmochim Acta* 67: 2173–2187
- Rubatto D, Hermann J (2007) Experimental zircon/melt and zircon/garnet trace element partitioning and implications for the geochronology of crustal rocks. *Chem Geol* 241: 38–61
- Rudnick RL and Gao S (2004) Composition of the Continental Crust. In: Holland HD, Turekian KK (eds) *The Crust, Treatise on Geochemistry* 3: 1–64. Elsevier, Amsterdam
- Trotet F, Vidal O, Jolivet L (2001) Exhumation of Syros and Sifnos metamorphic rocks (Cyclades, Greece): new constraints on the P-T paths. *Eur J Mineral* 13: 901–920
- Tsujimori T, Itaya T (1999) Blueschist-facies metamorphism during Paleozoic orogeny in southwestern Japan: phengite K-Ar ages of blueschist-facies tectonic blocks in a serpentinite mélange beneath Early Paleozoic Oeyama ophiolite. *Island Arc* 8: 190–205
- Watson EB, Harrison TM (2005) Zircon thermometer reveals minimum melting conditions on earliest Earth. *Science* 308: 841–844
- Whitehouse MJ, Platt JP (2003) Dating high-grade metamorphism – constraints from rare-earth elements in zircon and garnet. *Contrib Mineral Petrol* 145: 61–74

Electronic supplementary material S2. Oxygen isotopic compositions in zircons analyzed by SIMS.

Notes: (1) In the Mount (Tsujiomori), all KIM-5N & 5W were corrected by a factor of 0.17‰ as the average KIM-5W is 0.34‰ higher than KIM-5N.

(2) In the Mount (Tsujiomori), part of the session a linear trend was used for correction.

(3) All zircons of interest were calibrated by an average value of each bracket.

(4) The classification of zircons in jadeite from Osavama, Japan (type I vs. type II) is after Tsujiomori et al. (2005). We refer them to as h-type and iq-type in this study.

(5) KIM-5 vaue, 5.09‰, was taken after Valley (2003).

Filename	mount	sample	grain no	Remarks	¹⁶ O (cps)	¹⁸ O/ ¹⁶ O	2 S.E.	¹⁸ O raw KIM-5	¹⁸ O calib	2 S.D.
OSJ - Jadeite, Osayama, SW Japan										
(Date: 8/3/2005)										
20050803@1.asc		Tsujiomori_KIM-5W			2.52E+09	2.0167E-03	0.18	5.72		
20050803@2.asc		Tsujiomori_KIM-5W			2.53E+09	2.0173E-03	0.23	6.01		
20050803@3.asc		Tsujiomori_KIM-5W			2.53E+09	2.0172E-03	0.23	6.01		
20050803@4.asc		Tsujiomori_KIM-5N			2.57E+09	2.0167E-03	0.18	5.75		
20050803@5.asc		Tsujiomori_KIM-5N			2.56E+09	2.0168E-03	0.21	5.80		
20050803@6.asc		Tsujiomori_KIM-5N			2.56E+09	2.0164E-03	0.24	5.57		
		Mean (3N+3W)						5.81±0.35 (2 S.D.)		
20050803@7.asc		Tsujiomori OSJ #15_1		SHRIMP (#15-37), h-type (type I)	2.53E+09	2.0149E-03	0.21	4.82	4.09	0.42
20050803@8.asc		Tsujiomori_OSJ_#15_2		SHRIMP (#15-38), iq-type (type II)	2.49E+09	2.0173E-03	0.15	6.03	5.29	0.42
20050803@9.asc		Tsujiomori_OSJ_#11_1		SHRIMP (#11-3), iq-type (type II)	2.46E+09	2.0173E-03	0.23	6.02	5.29	0.42
20050803@10.asc		Tsujiomori OSJ #11_2		SHRIMP (#11-36), h-type (type I)	2.45E+09	2.0143E-03	0.21	4.56	3.83	0.42
20050803@11.asc		Tsujiomori_KIM-5N			2.41E+09	2.0164E-03	0.20	5.59		
20050803@12.asc		Tsujiomori_KIM-5W			2.40E+09	2.0175E-03	0.18	6.13		
		Mean (N+W)						5.86±0.77		
20050803@13.asc		Tsujiomori_OSJ_#11_3		SHRIMP (#11-7), iq-type (type II)	2.36E+09	2.0169E-03	0.19	5.85	5.05	0.53
20050803@14.asc		Tsujiomori_OSJ_#11_4		SHRIMP (#11-4), h-type (type I)	2.35E+09	2.0135E-03	0.25	4.13	3.33	0.53
20050803@15.asc		Tsujiomori_OSJ_#11_5		SHRIMP (#11-6), h-type (type I)	2.37E+09	2.0140E-03	0.23	4.37	3.57	0.53
20050803@16.asc		Tsujiomori_OSJ_#11_6		SHRIMP (#11-5), h-type (type I)	2.36E+09	2.0140E-03	0.22	4.41	3.61	0.53
20050803@17.asc		Tsujiomori_KIM-5N			2.37E+09	2.0167E-03	0.20	5.74		
20050803@18.asc		Tsujiomori_KIM-5W			2.37E+09	2.0174E-03	0.21	6.09		
		Mean (N+W)						5.91±0.49		
20050803@19.asc		Tsujiomori OSJ #1_1		SHRIMP (#1-1), h-type (type I)	2.38E+09	2.0141E-03	0.17	4.44	3.54	0.35
20050803@20.asc		Tsujiomori_OSJ_#1_2		SHRIMP (#1-2), h-type (type I)	2.49E+09	2.0138E-03	0.25	4.28	3.38	0.35
20050803@21.asc		Tsujiomori_OSJ_#7_1		SHRIMP (#7-33), h-type (type I)	2.56E+09	2.0146E-03	0.18	4.71	3.81	0.35
20050803@22.asc		Tsujiomori OSJ #7_2		SHRIMP (#7-35), h-type (type I)	2.58E+09	2.0140E-03	0.21	4.40	3.50	0.35
20050803@23.asc		Tsujiomori_KIM-5N			2.62E+09	2.0172E-03	0.23	5.99		
20050803@24.asc		Tsujiomori_KIM-5W			2.67E+09	2.0175E-03	0.15	6.14		
		Mean (N+W)						6.07±0.22		
20050803@25.asc		Tsujiomori_OSJ_#7_3		SHRIMP (#7-34), h-type (type I)	2.67E+09	2.0145E-03	0.21	4.64	3.67	0.29
20050803@26.asc		Tsujiomori_OSJ_#14_1		SHRIMP (#14-31), h-type (type I)	2.67E+09	2.0146E-03	0.22	4.71	3.74	0.29
20050803@27.asc		Tsujiomori_OSJ_#14_2		SHRIMP (#14-30), h-type (type I)	2.64E+09	2.0151E-03	0.23	4.96	4.00	0.29
20050803@28.asc		Tsujiomori_OSJ_#14_3		SHRIMP (#14-32), h-type (type I)	2.63E+09	2.0149E-03	0.22	4.83	3.86	0.29
20050803@29.asc		Tsujiomori_KIM-5N			2.75E+09	2.0170E-03	0.17	5.88		
20050803@30.asc		Tsujiomori_KIM-5W			2.89E+09	2.0176E-03	0.17	6.20		
		Mean (N+W)						6.04±0.44		
20050803@31.asc		Tsujiomori OSJ #14_4		SHRIMP (#14-28), h-type (type I)	2.95E+09	2.0144E-03	0.26	4.58	3.69	0.37
20050803@32.asc		Tsujiomori_OSJ_#14_5		SHRIMP (#14-29), h-type (type I)	2.99E+09	2.0153E-03	0.17	5.04	4.15	0.37
20050803@33.asc		Tsujiomori_OSJ_#14_6		h-type (type I)	3.05E+09	2.0156E-03	0.24	5.18	4.28	0.37
20050803@34.asc		Tsujiomori OSJ #14_7		h-type (type I)	3.06E+09	2.0149E-03	0.10	4.85	3.95	0.37
20050803@35.asc		Tsujiomori_KIM-5N			3.02E+09	2.0168E-03	0.20	5.79		
20050803@36.asc		Tsujiomori_KIM-5W			2.48E+09	2.0174E-03	0.23	6.07		
		Mean (N+W)						5.93±0.39		
20050803@37.asc		Tsujiomori_OSJ_#10_1		SHRIMP (#10-24), h-type (type I)	2.50E+09	2.0148E-03	0.19	4.79	3.95	0.43
20050803@38.asc		Tsujiomori_OSJ_#10_2		SHRIMP (#10-27), h-type (type I)	2.54E+09	2.0151E-03	0.15	4.92	4.09	0.43
20050803@39.asc		Tsujiomori OSJ #10_3		SHRIMP (#10-26), h-type (type I)	2.54E+09	2.0148E-03	0.23	4.79	3.95	0.43
20050803@40.asc		Tsujiomori_OSJ_#10_4		SHRIMP (#10-25), h-type (type I)	2.61E+09	2.0144E-03	0.19	4.58	3.74	0.43
20050803@41.asc		Tsujiomori_KIM-5N			2.68E+09	2.0166E-03	0.23	5.70		
20050803@42.asc		Tsujiomori_KIM-5W			2.80E+09	2.0175E-03	0.16	6.15		
		Mean (N+W)						5.92±0.62		
20050803@43.asc		Tsujiomori OSJ #9_1		SHRIMP (#9-14), h-type (type I)	2.83E+09	2.0153E-03	0.27	5.04	4.18	0.57
20050803@44.asc		Tsujiomori_OSJ_#9_2		SHRIMP (#9-21 (3A-1)), h-type (typ	2.86E+09	2.0156E-03	0.17	5.19	4.33	0.57
20050803@45.asc		Tsujiomori_OSJ_#9_3		SHRIMP (#9-22 (3A-2)), h-type (typ	2.90E+09	2.0152E-03	0.17	5.00	4.14	0.57
20050803@46.asc		Tsujiomori OSJ #9_4		h-type (type I)	2.89E+09	2.0152E-03	0.26	4.97	4.11	0.57
20050803@47.asc		Tsujiomori_KIM-5N			2.90E+09	2.0167E-03	0.20	5.71		
20050803@48.asc		Tsujiomori_KIM-5W			2.89E+09	2.0177E-03	0.15	6.25		
		Mean (N+W)						5.98±0.75		
20050803@49.asc		Tsujiomori_OSJ_#9_5		SHRIMP (#9-16?), h-type (type I)	2.84E+09	2.0154E-03	0.23	5.08	4.28	0.62
20050803@50.asc		Tsujiomori_OSJ_#9_6		SHRIMP (#9-23 (3A-8)), h-type (typ	2.85E+09	2.0154E-03	0.25	5.07	4.27	0.62
20050803@51.asc		Tsujiomori OSJ #9_7		SHRIMP (#9-17 (3A-7)), h-type (typ	2.90E+09	2.0149E-03	0.21	4.86	4.06	0.62
20050803@52.asc		Tsujiomori_OSJ_#9_8		SHRIMP (#9-19 (3A-5)), h-type (typ	2.93E+09	2.0149E-03	0.24	4.86	4.07	0.62
20050803@53.asc		Tsujiomori_KIM-5N			2.89E+09	2.0163E-03	0.16	5.55		
20050803@54.asc		Tsujiomori_KIM-5W			3.00E+09	2.0173E-03	0.19	6.03		
		Mean (N+W)						5.79±0.68		
20050803@55.asc		Tsujiomori OSJ #9_9		SHRIMP (#9-20 (3A-4)), h-type (typ	2.97E+09	2.0147E-03	0.16	4.75	3.98	0.62
20050803@56.asc		Tsujiomori_OSJ_#9_10		SHRIMP (#9-18 (3A-6)), h-type (typ	2.94E+09	2.0149E-03	0.21	4.85	4.07	0.62
20050803@57.asc		Tsujiomori_OSJ_#5_1		SHRIMP (#5-13), h-type (type I)	2.94E+09	2.0151E-03	0.18	4.95	4.18	0.62
20050803@58.asc		Tsujiomori OSJ #5_2		SHRIMP (#5-12), h-type (type I)	2.99E+09	2.0157E-03	0.19	5.21	4.44	0.62
20050803@59.asc		Tsujiomori_KIM-5N			2.98E+09	2.0166E-03	0.20	5.67		
20050803@60.asc		Tsujiomori_KIM-5W			3.04E+09	2.0177E-03	0.15	6.21		
		Mean (N+W)						5.94±0.77		
20050803@61.asc		Tsujiomori_OSJ_#5_3		SHRIMP (#5-11), h-type (type I)	3.09E+09	2.0145E-03	0.13	4.63	3.76	0.63
20050803@62.asc		Tsujiomori_OSJ_#5_4		SHRIMP (#5-9), h-type (type I)	3.10E+09	2.0145E-03	0.21	4.65	3.79	0.63
20050803@63.asc		Tsujiomori OSJ #5_5		SHRIMP (#5-10), h-type (type I)	3.18E+09	2.0147E-03	0.13	4.73	3.86	0.63
20050803@64.asc		Tsujiomori_OSJ_#5_6		SHRIMP (#5-8), h-type (type I)	3.16E+09	2.0143E-03	0.14	4.55	3.69	0.63
20050803@65.asc		Tsujiomori_KIM-5N			3.10E+09	2.0167E-03	0.20	5.72		
20050803@66.asc		Tsujiomori_KIM-5W			3.03E+09	2.0177E-03	0.18	6.24		
20050803@67.asc		Tsujiomori_KIM-5N			2.92E+09	2.0164E-03	0.19	5.59		
20050803@68.asc		Tsujiomori_KIM-5N			2.75E+09	2.0168E-03	0.19	5.78		
		Mean ((3N/3)+W)						5.83±0.56		
20050803@69.asc		Tsujiomori_OSJ_#11_1R		h-type (type I)	2.71E+09	2.0137E-03	0.23	4.23	3.30	0.41
20050803@70.asc		Tsujiomori OSJ #11C		iq-type (type II)	2.85E+09	2.0171E-03	0.17	5.92	4.98	0.41
20050803@71.asc		Tsujiomori_OSJ_#11R		h-type (type I)	3.00E+09	2.0138E-03	0.19	4.30	3.36	0.41
20050803@72.asc		Tsujiomori_OSJ_#11C		iq-type (type II)	3.09E+09	2.0173E-03	0.18	6.05	5.12	0.41
20050803@73.asc		Tsujiomori OSJ #11R		h-type (type I)	3.11E+09	2.0139E-03	0.19	4.33	3.39	0.41
20050803@74.asc		Tsujiomori_OSJ_#11C		iq-type (type II)	3.17E+09	2.0172E-03	0.16	5.98	5.04	0.41
20050803@75.asc		Tsujiomori_KIM-5N			3.22E+09	2.0169E-03	0.15	5.86		
20050803@76.asc		Tsujiomori_KIM-5N			3.25E+09	2.0169E-03	0.16	5.85		
20050803@77.asc		Tsujiomori_KIM-5N			3.16E+09	2.0172E-03	0.20	5.97		
		Mean (3N)						5.89±0.14		
20050803@78.asc		Tsujiomori OSJ #7R		h-type (type I)	3.11E+09	2.0147E-03	0.23	4.72	3.79	0.23
20050803@79.asc		Tsujiomori_OSJ_#7C		h-type (type I)	3.14E+09	2.0144E-03	0.23	4.58	3.65	0.23
20050803@80.asc		Tsujiomori_OSJ_#7R		h-type (type I)	3.13E+09	2.0141E-03	0.18	4.46	3.52	0.23
20050803@81.asc		Tsujiomori_OSJ_#7C		h-type (type I)	3.17E+09	2.0144E-03	0.17	4.60	3.67	0.23
20050803@82.asc		Tsujiomori_OSJ_#7R		h-type (type I)	3.29E+09	2.0144E-03	0.19	4.61	3.68	0.23
20050803@83.asc		Tsujiomori OSJ #7C		h-type (type I)	3.30E+09	2.0149E-03	0.2			

Electronic supplementary material S2. Oxygen isotopic compositions in zircons analyzed by SIMS.

Notes: (1) In the Mount (Tsujimori), all KIM-5N & 5W were corrected by a factor of 0.17‰ as the average KIM-5W is 0.34‰ higher than KIM-5N.

(2) In the Mount (Tsujimori), part of the session a linear trend was used for correction.

(3) All zircons of interest were calibrated by an average value of each bracket.

(4) The classification of zircons in jadeite from Osavama, Japan (type I vs. type II) is after Tsujimori et al. (2005). We refer them to as h-type and iq-type in this study.

(5) KIM-5 vauve, 5.09‰, was taken after Valley (2003).

Filename	mount	sample	grain	no	Remarks	¹⁶ O (cps)	¹⁸ O/ ¹⁶ O	2 S.E.	δ ¹⁸ O raw KIM-5	δ ¹⁸ O calib	2 S.D.
20050803@88.asc	Tsujimori	OSJ	#10C		h-type (type I)	2.73E+09	2.0144E-03	0.19	4.59	3.79	0.30
20050803@89.asc	Tsujimori	OSJ	#10R		h-type (type I)	2.80E+09	2.0143E-03	0.20	4.52	3.72	0.30
20050803@90.asc	Tsujimori	OSJ	#10C		h-type (type I)	2.80E+09	2.0149E-03	0.19	4.81	4.02	0.30
20050803@91.asc	Tsujimori	OSJ	#10R		h-type (type I)	2.75E+09	2.0147E-03	0.20	4.76	3.96	0.30
20050803@92.asc	Tsujimori	OSJ	#10C		h-type (type I)	2.67E+09	2.0145E-03	0.21	4.63	3.84	0.30
20050803@93.asc	Tsujimori	KIM	5N			2.66E+09	2.0163E-03	0.20	5.54		
20050803@94.asc	Tsujimori	KIM	5N			2.80E+09	2.0165E-03	0.18	5.62		
20050803@95.asc	Tsujimori	KIM	5N			2.83E+09	2.0166E-03	0.18	5.70		
					Mean (3N)				5.62±0.17		
20050803@96.asc	Tsujimori	OSJ	#6R		h-type (type I)	3.01E+09	2.0152E-03	0.24	5.00	4.15	0.35
20050803@97.asc	Tsujimori	OSJ	#6C		h-type (type I)	3.02E+09	2.0141E-03	0.17	4.46	3.61	0.35
20050803@98.asc	Tsujimori	OSJ	#6R		h-type (type I)	3.17E+09	2.0147E-03	0.20	4.74	3.90	0.35
20050803@99.asc	Tsujimori	OSJ	#6C		h-type (type I)	3.35E+09	2.0144E-03	0.12	4.58	3.74	0.35
20050803@100.asc	Tsujimori	OSJ	#6R		h-type (type I)	3.45E+09	2.0148E-03	0.14	4.77	3.92	0.35
20050803@101.asc	Tsujimori	OSJ	#6C		h-type (type I)	3.38E+09	2.0143E-03	0.20	4.55	3.70	0.35
20050803@102.asc	Tsujimori	KIM	5N			3.10E+09	2.0168E-03	0.15	5.80		
20050803@103.asc	Tsujimori	KIM	5N			3.16E+09	2.0168E-03	0.19	5.76		
20050803@104.asc	Tsujimori	KIM	5N			3.59E+09	2.0174E-03	0.14	6.07		
20050803@105.asc	Tsujimori	KIM	5N			2.69E+09	2.0170E-03	0.22	5.87		
					Mean (4N)				5.88±0.27		
20050803@106.asc	Tsujimori	OSJ	#13R**		h-type (type I)	2.84E+09	2.0141E-03	0.15	4.44	3.41	0.30
20050803@107.asc	Tsujimori	OSJ	#13R		h-type (type I)	2.82E+09	2.0144E-03	0.12	4.60	3.57	0.30
20050803@108.asc	Tsujimori	OSJ	#13C		h-type (type I)	2.87E+09	2.0137E-03	0.24	4.26	3.23	0.30
20050803@109.asc	Tsujimori	OSJ	#13R		h-type (type I)	2.94E+09	2.0143E-03	0.23	4.54	3.51	0.30
20050803@110.asc	Tsujimori	OSJ	#13C		h-type (type I)	3.04E+09	2.0139E-03	0.13	4.35	3.32	0.30
20050803@111.asc	Tsujimori	OSJ	#13R		h-type (type I)	3.01E+09	2.0146E-03	0.16	4.66	3.63	0.30
20050803@112.asc	Tsujimori	OSJ	#13C		h-type (type I)	3.09E+09	2.0140E-03	0.17	4.41	3.38	0.30
20050803@113.asc	Tsujimori	KIM	5N			3.04E+09	2.0170E-03	0.15	5.91		
20050803@114.asc	Tsujimori	KIM	5N			3.07E+09	2.0174E-03	0.11	6.09		
20050803@115.asc	Tsujimori	KIM	5N			3.14E+09	2.0175E-03	0.16	6.15		
					Mean (3N)				6.05±0.25		
20050803@116.asc	Tsujimori	OSJ	#9R		h-type (type I)	3.26E+09	2.0156E-03	0.22	5.20	3.97	0.36
20050803@117.asc	Tsujimori	OSJ	#9C		h-type (type I)	3.22E+09	2.0161E-03	0.12	5.44	4.21	0.36
20050803@118.asc	Tsujimori	OSJ	#9R		h-type (type I)	3.26E+09	2.0158E-03	0.18	5.29	4.07	0.36
20050803@119.asc	Tsujimori	OSJ	#9C		h-type (type I)	3.13E+09	2.0152E-03	0.13	5.01	3.79	0.36
20050803@120.asc	Tsujimori	OSJ	#9R		h-type (type I)	3.09E+09	2.0155E-03	0.19	5.12	3.90	0.36
20050803@121.asc	Tsujimori	OSJ	#9C		h-type (type I)	3.12E+09	2.0153E-03	0.14	5.06	3.84	0.36
20050803@122.asc	Tsujimori	KIM	5N			3.30E+09	2.0173E-03	0.15	6.03		
20050803@123.asc	Tsujimori	KIM	5N			3.62E+09	2.0182E-03	0.13	6.48		
20050803@124.asc	Tsujimori	KIM	5N			2.55E+09	2.0175E-03	0.18	6.13		
20050803@125.asc	Tsujimori	KIM	5N			2.90E+09	2.0177E-03	0.21	6.23		
					Mean (4N)				6.22±0.39		
20050803@126.asc	Tsujimori	OSJ	#9C		SHRIMP (#9-15 (3A-3)), h-type (typ	3.01E+09	2.0162E-03	0.18	5.48	4.12	0.68
20050803@127.asc	Tsujimori	OSJ	#9R		h-type (type I)	2.90E+09	2.0158E-03	0.23	5.30	3.94	0.68
20050803@128.asc	Tsujimori	KIM	5W			3.09E+09	2.0192E-03	0.16	6.97		
20050803@129.asc	Tsujimori	KIM	5W			3.08E+09	2.0188E-03	0.19	6.79		
20050803@130.asc	Tsujimori	KIM	5W			2.76E+09	2.0178E-03	0.20	6.27		
20050803@131.asc	Tsujimori	KIM	5W			2.60E+09	2.0186E-03	0.24	6.70		
					Mean (4W)				6.68±0.59		
20050803@132.asc	Tsujimori	OSJ	#15R		h-type (type I)	2.67E+09	2.0145E-03	0.31	4.62	3.51	0.94
20050803@133.asc	Tsujimori	OSJ	#15C		iq-type (type II)	2.11E+09	2.0170E-03	0.26	5.89	4.78	0.94
20050803@134.asc	Tsujimori	OSJ	#15X		iq-type (type II)	2.45E+09	2.0168E-03	0.23	5.77	4.66	0.94
20050803@135.asc	Tsujimori	OSJ	#15R		h-type (type I)	2.40E+09	2.0142E-03	0.21	4.47	3.36	0.94
20050803@136.asc	Tsujimori	OSJ	#15C		iq-type (type II)	2.35E+09	2.0166E-03	0.20	5.41	4.60	0.94
20050803@137.asc	Tsujimori	OSJ	#15X		iq-type (type II)	1.93E+09	2.0171E-03	0.33	5.95	4.84	0.94
20050803@138.asc	Tsujimori	OSJ	#15R		h-type (type I)	1.59E+09	2.0140E-03	0.33	4.38	3.27	0.94
20050803@139.asc	Tsujimori	OSJ	#15C		iq-type (type II)	2.55E+09	2.0170E-03	0.22	5.86	4.75	0.94
20050803@140.asc	Tsujimori	OSJ	#15X		iq-type (type II)	2.58E+09	2.0175E-03	0.19	6.16	5.04	0.94
20050803@141.asc	Tsujimori	KIM	5W			2.80E+09	2.0177E-03	0.14	6.22		
20050803@142.asc	Tsujimori	KIM	5W			2.96E+09	2.0172E-03	0.20	6.00		
20050803@143.asc	Tsujimori	KIM	5W			3.20E+09	2.0172E-03	0.14	5.97		
20050803@144.asc	Tsujimori	KIM	5N			3.24E+09	2.0165E-03	0.21	5.62		
20050803@145.asc	Tsujimori	KIM	5N			3.29E+09	2.0167E-03	0.20	5.72		
20050803@146.asc	Tsujimori	KIM	5N			3.42E+09	2.0169E-03	0.13	5.82		
					Mean all (3N+3W)				5.89±0.43		
20050803@147.asc	Tsujimori	OSJ	#11R		h-type (type I)	3.26E+09	2.0146E-03	0.18	4.68	3.84	0.35
20050803@148.asc	Tsujimori	OSJ	#11C		iq-type (type II)	2.97E+09	2.0172E-03	0.15	5.96	5.12	0.35
20050803@149.asc	Tsujimori	OSJ	#11R		h-type (type I)	2.91E+09	2.0142E-03	0.15	4.51	3.67	0.35
20050803@150.asc	Tsujimori	OSJ	#11C		iq-type (type II)	2.97E+09	2.0168E-03	0.19	5.79	4.94	0.35
20050803@151.asc	Tsujimori	OSJ	#11R		h-type (type I)	3.11E+09	2.0138E-03	0.15	4.31	3.47	0.35
20050803@152.asc	Tsujimori	OSJ	#11C		iq-type (type II)	3.21E+09	2.0169E-03	0.21	5.82	4.98	0.35
20050803@153.asc	Tsujimori	KIM	5N			3.26E+09	2.0167E-03	0.18	5.74		
20050803@154.asc	Tsujimori	KIM	5N			3.35E+09	2.0169E-03	0.13	5.81		
20050803@155.asc	Tsujimori	KIM	5N			3.42E+09	2.0169E-03	0.15	5.86		
					Mean (3N)				5.80±0.11		
20050803@156.asc	Tsujimori	OSJ	#11R		h-type (type I)	3.47E+09	2.0149E-03	0.16	4.83	3.97	0.16
20050803@157.asc	Tsujimori	OSJ	#11C		iq-type (type II)	3.34E+09	2.0175E-03	0.14	6.13	5.27	0.16
20050803@158.asc	Tsujimori	OSJ	#11R		h-type (type I)	3.28E+09	2.0137E-03	0.11	4.24	3.38	0.16
20050803@159.asc	Tsujimori	OSJ	#11C		iq-type (type II)	2.94E+09	2.0165E-03	0.21	5.66	4.80	0.16
20050803@160.asc	Tsujimori	OSJ	#11R		h-type (type I)	2.58E+09	2.0141E-03	0.23	4.45	3.59	0.16
20050803@161.asc	Tsujimori	OSJ	#11C		iq-type (type II)	2.43E+09	2.0169E-03	0.19	5.84	4.98	0.16
20050803@162.asc	Tsujimori	KIM	5N			2.43E+09	2.0166E-03	0.19	5.68		
20050803@163.asc	Tsujimori	KIM	5N			2.44E+09	2.0166E-03	0.22	5.71		
20050803@164.asc	Tsujimori	KIM	5N			2.44E+09	2.0170E-03	0.23	5.88		
					Mean (3N)				5.76±0.21		
20050803 chain@1.asc	Tsujimori	OSJ	#11		h-type (type I)	2.36E+09	2.0141E-03	0.23	4.42	3.59	0.35
20050803 chain@2.asc	Tsujimori	OSJ	#11		h-type (type I)	2.44E+09	2.0141E-03	0.29	4.44	3.60	0.35
20050803 chain@3.asc	Tsujimori	OSJ	#11		h-type (type I)	2.67E+09	2.0143E-03	0.21	4.53	3.70	0.35
20050803 chain@4.asc	Tsujimori	OSJ	#11		h-type (type I)	3.19E+09	2.0140E-03	0.18	4.38	3.55	0.35
20050803 chain@6.asc	Tsujimori	OSJ	#11		on core-rim boundary	3.45E+09	2.0155E-03	0.14	5.12	4.29	0.35
20050803 chain@7.asc	Tsujimori	OSJ	#11		h-type (type I)	3.49E+09	2.0134E-03	0.16	4.10	3.27	0.35
20050803 chain@8.asc	Tsujimori	OSJ	#11		iq-type (type II)	3.53E+09	2.0168E-03	0.18	5.76	4.93	0.35
20050803@165.asc	Tsujimori	OSJ	#11C		iq-type (type II)	3.32E+09	2.0168E-03	0.18	5.80	4.97	0.35
20050803@166.asc	Tsujimori	OSJ	#11R		h-type (type I)	3.26E+09	2.0133E-03	0.17	4.06	3.23	0.35
20050803@167.asc	Tsujimori	KIM	5N			3.32E+09	2.0170E-03	0.15	5.87		
20050803@168.asc	Tsujimori	KIM	5N			3.47E+09	2.0169E-03	0.14	5.83		
20050803@169.asc	Tsujimori	KIM	5N			3.60E+09	2.0171E-03	0.13	5.92		
20050803@170.asc	Tsujimori	KIM	5W			3.83E+09	2.0178E-03	0.15	6.28		
20050803@171.asc	Tsujimori	KIM	5W			2.55E+09	2.0168E-03	0.20	5.81		
20050803@172.asc	Tsujimori	KIM	5W			2.54E+09	2.0168E-03	0.15	5.78		
					Mean all (3N+3W)				5.92±0.37		
20050803@173.asc	Tsujimori	OSJ	#16R		h-type (type I)	2.48E+09	2.0150E-03	0.21	4.87	4.13	0.36

Electronic supplementary material S2. Oxygen isotopic compositions in zircons analyzed by SIMS.

Notes: (1) In the Mount (Tsujimori), all KIM-5N & 5W were corrected by a factor of 0.17‰ as the average KIM-5W is 0.34‰ higher than KIM-5N.

(2) In the Mount (Tsujimori), part of the session a linear trend was used for correction.

(3) All zircons of interest were calibrated by an average value of each bracket.

(4) The classification of zircons in jadeite from Osavama, Japan (type I vs. type II) is after Tsujimori et al. (2005). We refer them to as h-type and iq-type in this study.

(5) KIM-5 vaue, 5.09‰, was taken after Valley (2003).

Filename	mount	sample	grain	no	Remarks	¹⁶ O (cps)	¹⁸ O/ ¹⁶ O	2 S.E.	¹⁸ O raw KIM-5	¹⁸ O calib	2 S.D.
20050803@174.asc	Tsujimori	OSJ_#16M			h-type (type I)	2.47E+09	2.0149E-03	0.24	4.85	4.10	0.36
20050803@175.asc	Tsujimori	OSJ_#16C			h-type (type I)	2.53E+09	2.0148E-03	0.22	4.77	4.03	0.36
20050803@176.asc	Tsujimori	KIM-5W				2.63E+09	2.0168E-03	0.21	5.76		
20050803@177.asc	Tsujimori	KIM-5W				2.63E+09	2.0174E-03	0.23	6.08		
		Mean (3W)							5.92±0.45		
20050803@178.asc	Tsujimori	OSJ_#12R			h-type (type I)	2.61E+09	2.0145E-03	0.21	4.63	3.85	0.54
20050803@179.asc	Tsujimori	OSJ_#12C			h-type (type I)	2.60E+09	2.0149E-03	0.25	4.86	4.08	0.54
20050803@180.asc	Tsujimori	OSJ_#8R			iq-type (type II)	2.69E+09	2.0174E-03	0.19	6.09	5.32	0.54
20050803@181.asc	Tsujimori	OSJ_#8C			iq-type (type II)	2.85E+09	2.0174E-03	0.19	6.07	5.29	0.54
20050803@182.asc	Tsujimori	OSJ_#8			iq-type (type II)	2.94E+09	2.0172E-03	0.16	5.97	5.19	0.54
20050803@183.asc	Tsujimori	KIM-5N				3.06E+09	2.0166E-03	0.17	5.71		
20050803@184.asc	Tsujimori	KIM-5N				3.20E+09	2.0167E-03	0.14	5.71		
20050803@185.asc	Tsujimori	KIM-5W				3.39E+09	2.0179E-03	0.16	6.33		
20050803@186.asc	Tsujimori	KIM-5W				3.52E+09	2.0176E-03	0.17	6.18		
		Mean (2N+2W)							5.98±0.64		
20050803@187.asc	Tsujimori	OSJ_#8'R'			iq-type (type II)	3.44E+09	2.0176E-03	0.14	6.20	5.30	0.49
20050803@188.asc	Tsujimori	OSJ_#8R			iq-type (type II)	3.37E+09	2.0175E-03	0.18	6.15	5.25	0.49
20050803@189.asc	Tsujimori	OSJ_#3C			iq-type (type II)	3.31E+09	2.0171E-03	0.16	5.94	5.04	0.49
20050803@190.asc	Tsujimori	OSJ_#3R			h-type (type I)	3.34E+09	2.0149E-03	0.14	4.82	3.91	0.49
20050803@191.asc	Tsujimori	OSJ_#3R			iq-type (type II)	3.43E+09	2.0177E-03	0.17	6.25	5.35	0.49
20050803@192.asc	Tsujimori	OSJ_#3R			iq-type (type II)	3.39E+09	2.0177E-03	0.12	6.23	5.33	0.49
20050803@193.asc	Tsujimori	KIM-5N				3.38E+09	2.0167E-03	0.19	5.75		
20050803@194.asc	Tsujimori	KIM-5N				3.55E+09	2.0171E-03	0.16	5.93		
20050803@195.asc	Tsujimori	KIM-5W				3.61E+09	2.0175E-03	0.14	6.15		
20050803@196.asc	Tsujimori	KIM-5W				3.59E+09	2.0176E-03	0.18	6.17		
		Mean (2N+2W)							6.00±0.40		
MVE02-8-6 - Phengite jadeite, Guatemala											
(Date: 10/22/2005)											
20051022@1.asc	WF018	KIM-5A				2.47E+09	2.0166E-03	0.18	5.70		
20051022@2.asc	WF018	KIM-5A				2.46E+09	2.0163E-03	0.19	5.54		
20051022@3.asc	WF018	KIM-5B1				2.46E+09	2.0166E-03	0.29	5.71		
20051022@4.asc	WF018	KIM-5B2				2.45E+09	2.0167E-03	0.27	5.71		
									5.67±0.16		
20051022@5.asc	WF018	MVE02-8-6_Zrc1_1				2.49E+09	2.0169E-03	0.23	5.81	5.26	0.20
20051022@6.asc	WF018	MVE02-8-6_Zrc1_2				2.37E+09	2.0166E-03	0.30	5.69	5.14	0.20
20051022@7.asc	WF018	MVE02-8-6_Zrc1_3r				2.46E+09	2.0157E-03	0.22	5.26	4.71	0.20
20051022@8.asc	WF018	KIM-5A				2.46E+09	2.0162E-03	0.17	5.49		
20051022@9.asc	WF018	KIM-5B2				2.44E+09	2.0166E-03	0.17	5.69		
									5.59±0.29		
(Date: 10/26/2005)											
20051026@10.asc	WF018	KIM-5A				2.72E+09	2.0127E-03	0.30	3.73		
20051026@11.asc	WF018	KIM-5A				2.72E+09	2.0126E-03	0.17	3.69		
20051026@12.asc	WF018	KIM-5B2				2.75E+09	2.0125E-03	0.19	3.66		
20051026@13.asc	WF018	KIM-5B1			small grain	2.74E+09	2.0121E-03	0.16	3.42		
									3.63±0.28		
20051026@14.asc	WF018	MVE02-8-6_Zrc1_4				2.56E+09	2.0111E-03	0.17	2.93	4.45	0.27
20051026@15.asc	WF018	MVE02-8-6_Zrc1_5				2.66E+09	2.0114E-03	0.22	3.11	4.63	0.27
20051026@16.asc	WF018	KIM-5A				2.75E+09	2.0119E-03	0.16	3.37		
20051026@17.asc	WF018	KIM-5A				2.78E+09	2.0124E-03	0.20	3.58		
20051026@18.asc	WF018	KIM-5B2				2.75E+09	2.0125E-03	0.17	3.64		
20051026@19.asc	WF018	KIM-5B1				2.71E+09	2.0122E-03	0.29	3.48		
									3.52±0.24		
20051026@20.asc	WF018	MVE02-8-6_Zrc2_1				2.60E+09	2.0115E-03	0.19	3.14	4.69	0.24
20051026@21.asc	WF018	MVE02-8-6_Zrc2_2			among holes	2.53E+09	2.0098E-03	0.17	2.31	3.86	0.24
20051026@22.asc	WF018	KIM-5A				2.76E+09	2.0126E-03	0.19	3.70		
20051026@23.asc	WF018	KIM-5B2				2.81E+09	2.0122E-03	0.20	3.49		
									3.59±0.29		
20051026@24.asc	WF018	MVE02-8-6_Zrc3_1				2.74E+09	2.0128E-03	0.20	3.77	5.33	0.22
20051026@25.asc	WF018	MVE02-8-6_Zrc3_2				2.62E+09	2.0108E-03	0.19	2.77	4.33	0.22
20051026@26.asc	WF018	KIM-5A				2.79E+09	2.0121E-03	0.19	3.46		
20051026@27.asc	WF018	KIM-5B2				2.81E+09	2.0122E-03	0.16	3.48		
									3.47±0.04		
20051026@28.asc	WF018	MVE02-8-6_Zrc6_1				2.79E+09	2.0118E-03	0.16	3.27	4.96	0.20
20051026@29.asc	WF018	KIM-5A				2.80E+09	2.0120E-03	0.17	3.38		
20051026@30.asc	WF018	KIM-5B2				2.80E+09	2.0118E-03	0.16	3.27		
									3.32±0.16		
20051026@31.asc	WF018	KIM-5A				2.82E+09	2.0169E-03	0.13	5.86		
20051026@32.asc	WF018	KIM-5B2				2.83E+09	2.0169E-03	0.16	5.83		
									5.84±0.05		
20051026@33.asc	WF018	MVE02-8-6_Zrc5_1c				2.80E+09	2.0167E-03	0.18	5.74	5.03	0.15
20051026@34.asc	WF018	MVE02-8-6_Zrc5_2r				2.65E+09	2.0171E-03	0.16	5.92	5.20	0.15
20051026@35.asc	WF018	MVE02-8-6_Zrc4_1			edge!	2.57E+09	2.0154E-03	0.22	5.09	4.37	0.15
20051026@36.asc	WF018	MVE02-8-6_Zrc4_2			edge!	2.61E+09	2.0157E-03	0.18	5.25	4.53	0.15
20051026@37.asc	WF018	KIM-5A				2.84E+09	2.0169E-03	0.17	5.82		
20051026@38.asc	WF018	KIM-5A				2.84E+09	2.0168E-03	0.23	5.77		
20051026@39.asc	WF018	KIM-5A			btw 2 pits (10&11)	2.71E+09	2.0168E-03	0.20	5.77		
20051026@40.asc	WF018	KIM-5B2				2.83E+09	2.0169E-03	0.18	5.83		
20051026@41.asc	WF018	KIM-5B2				2.85E+09	2.0169E-03	0.18	5.84		
20051026@42.asc	WF018	KIM-5B2			among 3 pits (12&18&41))	2.71E+09	2.0170E-03	0.21	5.90		
20051026@43.asc	WF018	KIM-5B1				2.81E+09	2.0165E-03	0.21	5.64		
									5.80±0.16		
(Date: 3/31/2006)											
20060331@225.asc	WF018	KIM-5				2.12E+09		0.25	7.57		
20060331@226.asc	WF018	KIM-5A				2.07E+09		0.21	6.93		
20060331@227.asc	WF018	KIM-5A				2.20E+09		0.21	7.50		
20060331@228.asc	WF018	KIM-5A				2.21E+09		0.28	7.25		
20060331@229.asc	WF018	KIM-5A				2.19E+09		0.22	7.02		
									7.26±0.57		
20060331@230.asc	WF018	MVE02-8-6_Zrc1_1				2.17E+09		0.24	7.05	4.92	0.42
20060331@231.asc	WF018	MVE02-8-6_Zrc1_2				2.20E+09		0.23	7.19	5.06	0.42
20060331@232.asc	WF018	MVE02-8-6_Zrc1_3				2.18E+09		0.24	7.12	4.98	0.42
20060331@233.asc	WF018	MVE02-8-6_Zrc1_4				2.15E+09		0.21	6.59	4.46	0.42
20060331@234.asc	WF018	MVE02-8-6_Zrc1_5				2.23E+09		0.21	7.57	5.44	0.42
20060331@235.asc	WF018	MVE02-8-6_Zrc3_1				2.23E+09		0.19	6.79	4.66	0.42
20060331@236.asc	WF018	MVE02-8-6_Zrc3_2				2.22E+09		0.22	7.09	4.96	0.42
20060331@237.asc	WF018	MVE02-8-6_Zrc3_3			partly on previous pit	2.19E+09		0.23	6.55	4.42	0.42
20060331@238.asc	WF018	KIM-5A				2.21E+09		0.25	7.03		
20060331@239.asc	WF018	KIM-5A			charging	2.13E+09		0.26	7.20		
20060331@240.asc	WF018	KIM-5A				2.15E+09		0.24	7.32		
20060331@241.asc	WF018	KIM-5A				2.03E+09		0.26	7.10		

Electronic supplementary material S2. Oxygen isotopic compositions in zircons analyzed by SIMS.

Notes: (1) In the Mount (Tsujimori), all KIM-5N & 5W were corrected by a factor of 0.17‰ as the average KIM-5W is 0.34‰ higher than KIM-5N.
 (2) In the Mount (Tsujimori), part of the session a linear trend was used for correction.
 (3) All zircons of interest were calibrated by an average value of each bracket.
 (4) The classification of zircons in jadeite from Osavama, Japan (type I vs. type II) is after Tsujimori et al. (2005). We refer them to as h-type and iq-type in this study.
 (5) KIM-5 vaue, 5.09‰, was taken after Valley (2003).

Filename	mount	sample	grain	no	Remarks	¹⁶ O (cps)	¹⁸ O/ ¹⁶ O	2 S.E.	¹⁸ O raw KIM-5	¹⁸ O calib	2 S.D.
20060331@242.asc	WF018	KIM-5A				2.01E+09		0.26	7.19±0.25	7.29	
3148 - Jadeite, Syros, Greece											
(Date: 10/22/2005)											
20060525@95.asc		Broecker-1	KIM-5			2.92E+09	2.019913	0.000459		7.34	
20060525@96.asc		Broecker-1	KIM-5			2.91E+09	2.019522	0.00032		7.14	
20060525@97.asc		Broecker-1	KIM-5			2.89E+09	2.019058	0.000482		6.91	
20060525@98.asc		Broecker-1	KIM-5			2.89E+09	2.019603	0.000435		7.18	
20060525@99.asc		Broecker-1	3148_2_1r		SHRIMP (2.1)	2.91E+09	2.019587	0.000375		7.18	5.18 0.34
20060525@100.asc		Broecker-1	3148_2_2c			2.89E+09	2.02005	0.000492		7.41	5.41 0.34
20060525@101.asc		Broecker-1	3148_4_1c			2.92E+09	2.019783	0.000319		7.27	5.28 0.34
20060525@102.asc		Broecker-1	3148_4_2r			2.79E+09	2.019134	0.000404		6.95	4.95 0.34
20060525@103.asc		Broecker-1	3148_6_1c		SHRIMP (6.1)	2.90E+09	2.019593	0.000326		7.18	5.18 0.34
20060525@104.asc		Broecker-1	3148_6_2c			2.90E+09	2.020032	0.000258		7.40	5.40 0.34
20060525@105.asc		Broecker-1	3148_6_3r			2.90E+09	2.019212	0.000399		6.99	4.99 0.34
20060525@106.asc		Broecker-1	3148_7_1r		SHRIMP (7.1)	2.88E+09	2.019445	0.000365		7.10	5.11 0.34
20060525@107.asc		Broecker-1	3148_7_2c		disturbed CL - data rejected	2.89E+09	2.01917	0.00036		6.97	4.97 0.34
20060525@108.asc		Broecker-1	3148_8_1r		SHRIMP (8.1)	2.89E+09	2.018948	0.000394		6.86	4.86 0.34
20060525@109.asc		Broecker-1	3148_8_2c		disturbed CL - data rejected	2.73E+09	2.01711	0.000427		5.94	3.94 0.34
20060525@110.asc		Broecker-1	3148_8_3r		inclusion? - data rejected	2.68E+09	2.016938	0.000489		5.85	3.86 0.34
20060525@111.asc		Broecker-1	3148_10_1r		SHRIMP (10.1)	2.69E+09	2.018464	0.000369		6.62	4.62 0.34
20060525@112.asc		Broecker-1	3148_10_2c		disturbed CL - data rejected	2.83E+09	2.017344	0.000672		6.06	4.06 0.34
20060525@113.asc		Broecker-1	3148_9_1r		SHRIMP (9.1)	2.89E+09	2.018784	0.000393		6.77	4.78 0.34
20060525@114.asc		Broecker-1	3148_9_2r			2.87E+09	2.019266	0.000329		7.02	5.02 0.34
20060525@115.asc		Broecker-1	3148_9_3r		disturbed CL core - data rejected	2.77E+09	2.015849	0.000543		5.31	3.31 0.34
20060525@116.asc		Broecker-1	KIM-5			2.90E+09	2.019313	0.000392		7.04	
20060525@117.asc		Broecker-1	KIM-5			2.89E+09	2.018857	0.000372		6.81	
20060525@118.asc		Broecker-1	KIM-5			2.90E+09	2.019331	0.000391		7.05	
20060525@119.asc		Broecker-1	KIM-5			2.90E+09	2.019688	0.000432		7.23	
20060525@120.asc		Broecker-1	3148_8_4r			2.90E+09	2.019929	0.000441		7.35	5.38 0.24
20060525@121.asc		Broecker-1	3148_8_5r			2.89E+09	2.02005	0.000396		7.41	5.44 0.24
20060525@122.asc		Broecker-1	3148_12_1r		SHRIMP (12.1)	2.90E+09	2.019876	0.000278		7.32	5.35 0.24
20060525@123.asc		Broecker-1	3148_12_2c			2.91E+09	2.019851	0.000428		7.31	5.34 0.24
20060525@124.asc		Broecker-1	3148_12_3c			2.91E+09	2.019558	0.000412		7.16	5.19 0.24
20060525@125.asc		Broecker-1	3148_14_1r		SHRIMP (14.1)	2.91E+09	2.019593	0.000437		7.18	5.21 0.24
20060525@126.asc		Broecker-1	3148_14_2r			2.91E+09	2.019845	0.00047		7.30	5.34 0.24
20060525@127.asc		Broecker-1	3148_15B_1r		SHRIMP (15B.1)	2.89E+09	2.020099	0.000306		7.43	5.46 0.24
20060525@128.asc		Broecker-1	3148_15B_2c			2.89E+09	2.019714	0.000359		7.24	5.27 0.24
20060525@129.asc		Broecker-1	3148_15A_1c			2.91E+09	2.019202	0.000316		6.98	5.02 0.24
20060525@130.asc		Broecker-1	3148_15A_2c			2.87E+09	2.019232	0.000318		7.00	5.03 0.24
20060525@131.asc		Broecker-1	3148_16_1c		SHRIMP (16.1)	2.86E+09	2.020095	0.000322		7.43	5.46 0.24
20060525@132.asc		Broecker-1	3148_19_1r		SHRIMP (19.2)	2.71E+09	2.019094	0.000377		6.93	4.96 0.24
20060525@133.asc		Broecker-1	3148_19_2c		SHRIMP (19C.1)	2.88E+09	2.019678	0.000509		7.22	5.25 0.24
20060525@134.asc		Broecker-1	3148_20_1c		SHRIMP (20.1)	2.88E+09	2.01949	0.000405		7.13	5.16 0.24
20060525@135.asc		Broecker-1	3148_20_2r			2.71E+09	2.018765	0.000494		6.77	4.80 0.24
20060525@136.asc		Broecker-1	KIM-5			2.87E+09	2.019298	0.000579		7.03	
20060525@137.asc		Broecker-1	KIM-5			2.89E+09	2.019459	0.000347		7.11	
20060525@138.asc		Broecker-1	KIM-5			2.89E+09	2.019503	0.000424		7.13	
20060525@139.asc		Broecker-1	KIM-5			2.89E+09	2.019365	0.000369		7.06	
3152A - Chlorite-actinolite schist, Syros, Greece											
20060525@140.asc		Broecker-1	3152A_1_1c		SHRIMP (1C.1)	2.90E+09	2.019974	0.000367		7.37	5.38 0.20
20060525@141.asc		Broecker-1	3152A_1_2r		SHRIMP (1.1)	2.90E+09	2.020031	0.000448		7.40	5.41 0.20
20060525@142.asc		Broecker-1	3152A_3_1r		SHRIMP (3.1)	2.89E+09	2.0194	0.000326		7.08	5.10 0.20
20060525@143.asc		Broecker-1	3152A_4_1r		SHRIMP (4.1)	2.89E+09	2.0195	0.000299		7.13	5.15 0.20
20060525@144.asc		Broecker-1	3152A_4_2r			2.89E+09	2.019692	0.000389		7.23	5.24 0.20
20060525@145.asc		Broecker-1	3152A_23_1r		SHRIMP (23.1)	2.90E+09	2.020004	0.00042		7.38	5.40 0.20
20060525@146.asc		Broecker-1	3152A_23_2c			2.89E+09	2.01943	0.000457		7.10	5.11 0.20
20060525@147.asc		Broecker-1	3152A_6A_1c		SHRIMP (6A.1)	2.90E+09	2.020009	0.000373		7.39	5.40 0.20
20060525@148.asc		Broecker-1	3152A_7_1r		SHRIMP (7.1)	2.89E+09	2.019493	0.000381		7.13	5.14 0.20
20060525@149.asc		Broecker-1	3152A_8_1r		SHRIMP (8.1)	2.89E+09	2.019387	0.000338		7.08	5.09 0.20
20060525@150.asc		Broecker-1	3152A_11_1r		SHRIMP (11.1)	2.90E+09	2.019259	0.000379		7.01	5.03 0.20
20060525@151.asc		Broecker-1	3152A_13_1r		SHRIMP (13.1)	2.90E+09	2.019407	0.000322		7.09	5.10 0.20
20060525@152.asc		Broecker-1	3152A_13_2r			2.89E+09	2.019296	0.000344		7.03	5.05 0.20
20060525@153.asc		Broecker-1	3152A_15_1r		SHRIMP (15.1)	2.90E+09	2.019774	0.000293		7.27	5.28 0.20
20060525@154.asc		Broecker-1	3152A_15_2c			2.90E+09	2.019176	0.000457		6.97	4.99 0.20
20060525@155.asc		Broecker-1	3152A_15_3r			2.90E+09	2.019753	0.000467		7.26	5.27 0.20
20060525@156.asc		Broecker-1	3152A_17_1r		SHRIMP (17.1)	2.73E+09	2.019516	0.00052		7.14	5.16 0.20
20060525@157.asc		Broecker-1	3152A_17_2r			2.89E+09	2.019336	0.000329		7.05	5.07 0.20
20060525@158.asc		Broecker-1	3152A_17_3c			2.90E+09	2.019983	0.000308		7.37	5.39 0.20
20060525@159.asc		Broecker-1	3152A_18_1c		SHRIMP (18.1)	2.90E+09	2.019794	0.000395		7.28	5.29 0.20
20060525@160.asc		Broecker-1	KIM-5			2.90E+09	2.019525	0.000441		7.14	
20060525@161.asc		Broecker-1	KIM-5			2.89E+09	2.019354	0.000428		7.06	
20060525@162.asc		Broecker-1	KIM-5			2.88E+09	2.018968	0.000395		6.87	
20060525@163.asc		Broecker-1	KIM-5			2.89E+09	2.0196	0.00039		7.18	
3149 - Omphacite, Syros, Greece											
(Date 6/8/2006)											
20060608@202.asc		Broecker-3	KIM-5			2.87E+09	2.01857	0.00053		6.67	
20060608@203.asc		Broecker-3	KIM-5			2.85E+09	2.01831	0.000457		6.54	
20060608@204.asc		Broecker-3	KIM-5			2.83E+09	2.018746	0.000459		6.76	
20060608@205.asc		Broecker-3	KIM-5			2.84E+09	2.018765	0.000505		6.77	
20060608@206.asc		Broecker-3	3149_7_1c		SHRIMP (7.1)	2.82E+09	2.019444	0.000463		7.10	5.44 0.22
20060608@207.asc		Broecker-3	3149_7_2r			2.83E+09	2.018707	0.00041		6.74	5.07 0.22
20060608@208.asc		Broecker-3	3149_7_3r			2.75E+09	2.018552	0.000518		6.66	5.00 0.22
20060608@209.asc		Broecker-3	3149_10_1c		SHRIMP (10.1)	2.84E+09	2.0194	0.000437		7.08	5.42 0.22
20060608@210.asc		Broecker-3	3149_10_2r			2.79E+09	2.018367	0.000458		6.57	4.90 0.22
20060608@211.asc		Broecker-3	3149_15_1r		SHRIMP (15.1)	2.83E+09	2.018377	0.000486		6.57	4.91 0.22
20060608@212.asc		Broecker-3	3149_15_2r			2.83E+09	2.018581	0.000357		6.67	5.01 0.22
20060608@213.asc		Broecker-3	3149_17_1c		SHRIMP (17.1)	2.83E+09	2.019529	0.000392		7.15	5.48 0.22
20060608@214.asc		Broecker-3	3149_18_1r (low)		SHRIMP (18.1)	2.64E+09	2.018745	0.000528		6.76	5.09 0.22
20060608@215.asc		Broecker-3	3149_19_1c		SHRIMP (19.1)	2.83E+09	2.018977	0.000437		6.87	5.21 0.22
20060608@216.asc		Broecker-3	3149_19_2r			2.83E+09	2.019243	0.000462		7.00	5.34 0.22
200											

Electronic supplementary material S2. Oxygen isotopic compositions in zircons analyzed by SIMS.

Notes: (1) In the Mount (Tsujimori), all KIM-5N & 5W were corrected by a factor of 0.17‰ as the average KIM-5W is 0.34‰ higher than KIM-5N.

(2) In the Mount (Tsujimori), part of the session a linear trend was used for correction.

(3) All zircons of interest were calibrated by an average value of each bracket.

(4) The classification of zircons in jadeite from Osavama, Japan (type I vs. type II) is after Tsujimori et al. (2005). We refer them to as h-type and iq-type in this study.

(5) KIM-5 vaue, 5.09‰, was taken after Valley (2003).

Filename	mount	sample	grain no	Remarks	¹⁶ O (cps)	¹⁸ O/ ¹⁶ O	2 S.E.	δ ¹⁸ O raw KIM-5	δ ¹⁸ O calib	2 S.D.
20060608@221.asc	Broecker-3	KIM-5			2.82E+09	2.018766	0.000503	6.77		
20060608@222.asc	Broecker-3	KIM-5			2.82E+09	2.018875	0.000469	6.82		
								6.82±0.07		
3151 - Glauconite, Syros, Greece										
20060608@223.asc	Broecker-3	3151_6_1c		SHRIMP (6.2)	2.84E+09	2.019382	0.000415	7.07	5.29	0.25
20060608@224.asc	Broecker-3	3151_6_2r		SHRIMP (6.1)	2.83E+09	2.01917	0.00048	6.97	5.19	0.25
20060608@225.asc	Broecker-3	3151_6_3r			2.84E+09	2.019674	0.000383	7.22	5.44	0.25
20060608@226.asc	Broecker-3	3151_7_1c		SHRIMP (7.1)	2.84E+09	2.019677	0.000544	7.22	5.44	0.25
20060608@227.asc	Broecker-3	3151_7_2r		SHRIMP (7.2)	2.83E+09	2.019816	0.000448	7.29	5.51	0.25
20060608@228.asc	Broecker-3	3151_9_1c		SHRIMP (9.1)	2.84E+09	2.019263	0.000442	7.01	5.23	0.25
20060608@229.asc	Broecker-3	3151_16A_1c		SHRIMP (16A.1)	2.82E+09	2.019643	0.00044	7.20	5.42	0.25
20060608@230.asc	Broecker-3	3151_16A_2r		SHRIMP (16A.2)	2.82E+09	2.018851	0.000358	6.81	5.03	0.25
20060608@231.asc	Broecker-3	3151_17_1r		SHRIMP (17.1)	2.81E+09	2.019052	0.000461	6.91	5.13	0.25
20060608@232.asc	Broecker-3	3151_17_2r			2.81E+09	2.018965	0.000396	6.87	5.09	0.25
20060608@233.asc	Broecker-3	3151_20_1c/r		SHRIMP (20.1)	2.83E+09	2.018756	0.000461	6.76	4.98	0.25
20060608@234.asc	Broecker-3	3151_20_2r/c		SHRIMP (20.2)	2.82E+09	2.019798	0.000402	7.28	5.50	0.25
20060608@235.asc	Broecker-3	KIM-5			2.82E+09	2.019369	0.000472	7.07		
20060608@236.asc	Broecker-3	KIM-5			2.81E+09	2.019318	0.000498	7.04		
20060608@237.asc	Broecker-3	KIM-5			2.81E+09	2.018704	0.00043	6.73		
20060608@238.asc	Broecker-3	KIM-5			2.80E+09	2.018871	0.000527	6.82		
								6.91±0.33		
3152B - Chlorite-actinolite schist, Syros, Greece										
20060608@239.asc	Broecker-3	3152B_3_1c/r		SHRIMP (3.1)	2.80E+09	2.019173	0.000432	6.97	5.18	0.27
20060608@240.asc	Broecker-3	3152B_3_2r			2.82E+09	2.019252	0.000488	7.01	5.22	0.27
20060608@241.asc	Broecker-3	3152B_4A_1c		SHRIMP (4A.1)	2.81E+09	2.019243	0.000362	7.00	5.22	0.27
20060608@242.asc	Broecker-3	3152B_4A_2r		SHRIMP (4A.2)	2.82E+09	2.018821	0.00047	6.79	5.01	0.27
20060608@243.asc	Broecker-3	3152B_7_1r		SHRIMP (7.1)	2.80E+09	2.018691	0.000288	6.73	4.94	0.27
20060608@244.asc	Broecker-3	3152B_7_2c		SHRIMP (7.2) disturbed CL core	2.79E+09	2.019058	0.00035	6.91	5.13	0.27
20060608@245.asc	Broecker-3	3152B_9B_1c		SHRIMP (9B.1)	2.78E+09	2.018993	0.000529	6.88	5.10	0.27
20060608@246.asc	Broecker-3	3152B_9_1c		SHRIMP (9.1)	2.79E+09	2.019063	0.000272	6.91	5.13	0.27
20060608@247.asc	Broecker-3	3152B_9_2c/r (low		SHRIMP (9.2)	2.56E+09	2.019163	0.00041	6.96	5.18	0.27
20060608@248.asc	Broecker-3	3152B_12_1c/r		SHRIMP (12.1)	2.77E+09	2.019119	0.000471	6.94	5.16	0.27
20060608@249.asc	Broecker-3	3152B_12_2c			2.76E+09	2.019206	0.000396	6.99	5.20	0.27
20060608@250.asc	Broecker-3	3152B_16_1c		SHRIMP (16.1)	2.77E+09	2.01874	0.000451	6.75	4.97	0.27
20060608@251.asc	Broecker-3	3152B_16_2r			2.75E+09	2.018954	0.000421	6.86	5.08	0.27
20060608@252.asc	Broecker-3	KIM-5			2.78E+09	2.019047	0.000575	6.91		
20060608@253.asc	Broecker-3	KIM-5			2.78E+09	2.019086	0.000524	6.93		
20060608@254.asc	Broecker-3	KIM-5			2.78E+09	2.018776	0.000416	6.77		
20060608@255.asc	Broecker-3	KIM-5			2.79E+09	2.01869	0.000443	6.73		
								6.83±0.20		

References:

Tsujimori T, Liou JG, Wooden J, Miyamoto T (2005) U-Pb dating of large zircons in low-temperature jadeite from the Osayama serpentinite mélange, SW Japan: insights into the timing of serpentinization. *Int Geol Rev* 47: 1048–1057
 Valley JW (2003) Oxygen isotopes in zircon. In: Hancher JM, Hoskin PWO (eds) *Zircon*, *Rev Mineral Geochem* 53: 343–385. Mineralogical Society of America/Geochemical Society, Washington, DC

Electronic supplementary material S3. Titanium concentrations in zircons analyzed by SIMS.

Ti-in-zircon temperatures were estimated based on the calibration of Watson and Harrison (2005) and Watson et al. (2006).
For mounts (Broecker 1 & 3), Au-coat removed after O-analysis so that O-pits may be contaminated in Ti.
The classification of zircons in jadelite from Osayama, Japan (type I vs. type II) is after Tsujimori et al. (2005).

Filename	mount_sample_grain_no	Ti ppm	T (Ti-in-zircon), °C	Remarks
<u>Okayama, SW Japan</u>				
20050811@95.asc	Tsujimori_KIM-5N	4.8	681	standard
20050811@96.asc	Tsujimori_KIM-5N	8.4	726	standard
20050811@97.asc	Tsujimori_KIM-5W	4.4	674	standard
20050811@98.asc	Tsujimori_OSJ_#15_a © (O-133, 136, 139)	1.2	586	ig-type (type II)
20050811@99.asc	Tsujimori_OSJ_#15_b ® (O-132, 135, 138)	2.7	638	h-type (type I)
20050811@100.asc	Tsujimori_OSJ_#15_c ® (O-134, 137, 140)	1.0	571	iq-type (type II)
20050811@101.asc	Tsujimori_OSJ_#15_d © (O-8)	1.2	585	iq-type (type II)
20050811@102.asc	Tsujimori_OSJ_#15_e ® (O-7)	2.9	642	h-type (type I)
20050811@103.asc	Tsujimori_OSJ_#11_a © (O-70, 72, 74)	2.6	634	ig-type (type II)
20050811@104.asc	Tsujimori_OSJ_#11_b ® (O-69, 71, 73, 14)	7.8	720	h-type (type I)
20050811@105.asc	Tsujimori_OSJ_#11_c © (O-148, 150, 152)	3.2	651	iq-type (type II)
20050811@106.asc	Tsujimori_OSJ_#11_d ® (O-147, 149, 151, 16)	6.3	702	h-type (type I)
20050811@107.asc	Tsujimori_OSJ_#11_e © (O-157, 159, 161)	2.6	636	ig-type (type II)
20050811@108.asc	Tsujimori_OSJ_#11_f ® (O-156, 158, 160, 10)	4.9	682	h-type (type I)
20050811@109.asc	Tsujimori_OSJ_#8_a ®/© (O-180)	2.6	635	ig-type (type II)
20050811@110.asc	Tsujimori_OSJ_#8_b © (O-181)	2.5	631	iq-type (type II)
20050811@111.asc	Tsujimori_OSJ_#8_c ®/® (O-182)	1.8	611	iq-type (type II)
20050811@112.asc	Tsujimori_OSJ_#8_d ® (O-187)	1.2	586	ig-type (type II)
20050811@113.asc	Tsujimori_OSJ_#8_e ® (O-188)	3.1	647	ig-type (type II)
20050811@114.asc	Tsujimori_OSJ_#3_a © (O-189)	2.2	622	ig-type (type II)
20050811@115.asc	Tsujimori_OSJ_#3_b ®/© (O-190)	4.6	677	h-type (type I)
20050811@116.asc	Tsujimori_OSJ_#3_c ® (O-191)	2.2	624	iq-type (type II)
20050811@117.asc	Tsujimori_OSJ_#3_d ©	1.9	615	ig-type (type II)
20050811@118.asc	Tsujimori_OSJ_#7_a ® (O-78, 80, 82)	5.1	685	h-type (type I)
20050811@119.asc	Tsujimori_OSJ_#7_b © (O-79, 81, 83)	3.8	663	h-type (type I)
20050811@120.asc	Tsujimori_OSJ_#9_a ® (O-116, 118, 120)	2.9	644	h-type (type I)
20050811@121.asc	Tsujimori_OSJ_#9_b © (O-117, 119, 121)	2.3	628	h-type (type I)
20050811@122.asc	Tsujimori_OSJ_#10_a ® (O-37, 87, 89, 91)	7.7	719	h-type (type I)
20050811@123.asc	Tsujimori_OSJ_#10_b © (O-88, 90, 92)	5.0	683	h-type (type I)
<u>Guatemala</u>				
20060915@71.asc	WF018_KIM-5A	4.2	671	standard
20060915@72.asc	WF018_MVE02-8-6_Zrc6_1	16.5	787	
20060915@73.asc	WF018_MVE02-8-6_Zrc5_1	17.8	794	
20060915@74.asc	WF018_MVE02-8-6_Zrc3_1 (overlap O-3)	4.5	676	
20060915@75.asc	WF018_KIM-5A	4.2	670	standard
20060915@76.asc	WF018_KIM-5A (overlap O-pit)	4.0	666	standard
20060915@77.asc	WF018_MVE02-8-6_Zrc2-1 (overlap O-1,2)	8.9	731	
20060915@78.asc	WF018_MVE02-8-6_Zrc1_1 (overlap O-1,2; inclusions?)	240.4	1127	
20060915@79.asc	WF018_MVE02-8-6_Zrc1-2 (overlap O-3,4)	18.1	796	
20060915@80.asc	WF018_MVE02-8-6_Zrc1-3 (overlap O-5)	10.4	745	
<u>Syros, Greece</u>				
20060919@17.asc	Broecker-1_KIM-5, new surface	4.4	673	standard
20060919@18.asc	Broecker-1_KIM-5, overlap O-pit	4.2	671	standard
20060919@19.asc	Broecker-1_3148_2_1 (O-2_2c)	14.0	772	
20060919@20.asc	Broecker-1_3148_2_2 (O-2_1r, U-2.1)	6.3	702	
20060919@21.asc	Broecker-1_3148_2_3, new surface	12.6	762	
20060919@22.asc	Broecker-1_3148_4-1 (O-4_1c)	12.7	762	
20060919@23.asc	Broecker-1_3148_4-2 (O-4_2r)	6.4	704	
20060919@24.asc	Broecker-1_3148_6_1 (O-6_1c, U-6.1)	7.9	720	
20060919@25.asc	Broecker-1_3148_6_2 (O-6_2c)	8.1	722	
20060919@26.asc	Broecker-1_3148_7_1 (O-7_1r, U-7.1)	7.8	720	
20060919@27.asc	Broecker-1_3148_7_2 (O-7_2c)	8.5	727	
20060919@28.asc	Broecker-1_3148_8_1 (O-8_1r, U-8.1)	9.5	736	
20060919@29.asc	Broecker-1_3148_8_2 (O-8_5r)	9.3	735	
20060919@30.asc	Broecker-1_3148_10_1 (O-10_1r, U-10.1)	4.2	669	
20060919@31.asc	Broecker-1_3148_9_1 (O-9_1r, U-9.1)	8.2	724	
20060919@32.asc	Broecker-1_3148_12_1 (O-12_1r, U-12.1)	9.6	737	
20060919@33.asc	Broecker-1_3148_14_1 (O-14_1r, U-14.1)	8.8	730	
20060919@34.asc	Broecker-1_3148_15B_1 (O-15B_1r, U-15B.1)	12.6	762	
20060919@35.asc	Broecker-1_3148_15B_2 (O-15B_2c)	7.0	711	
20060919@36.asc	Broecker-1_3148_15A_1 (O-15A_1c)	8.8	730	
20060919@37.asc	Broecker-1_3148_16_1 (O-16_1c, U-16.1)	12.6	761	
20060919@38.asc	Broecker-1_3148_19_1 (O-19_1r, U-19.2)	8.4	726	
20060919@39.asc	Broecker-1_3148_19_2 (O-19_2c, U-19C.1)	14.3	773	
20060919@40.asc	Broecker-1_3148_20_1 (O-20_1c, U-20.1)	10.5	746	
20060919@41.asc	Broecker-1_KIM-5, overlap O-pit	4.3	672	standard
20060919@42.asc	Broecker-1_3152A_1_1 (O-1_1c, U-1C.1)	12.4	760	
20060919@43.asc	Broecker-1_3152A_1_2 (O-1_2r, U-1.1)	12.7	762	
20060919@44.asc	Broecker-1_3152A_3_1 (O-3_1r, U-3.1)	4.7	679	
20060919@45.asc	Broecker-1_3152A_23_1 (O-23_1r, U-23.1)	9.4	735	
20060919@46.asc	Broecker-1_3152A_23_2 (O-23_2c)	14.0	772	
20060919@47.asc	Broecker-1_3152A_4_1 (O-4_1r, U-4.1)	10.6	746	
20060919@48.asc	Broecker-1_3152A_6A_1 (O-6A_1c, U-6A.1)	14.1	772	
20060919@49.asc	Broecker-1_3152A_7_1 (O-7_1r, U-7.1)	6.8	708	
20060919@50.asc	Broecker-1_3152A_8_1 (O-8_1r, U-8.1)	5.2	687	
20060919@51.asc	Broecker-1_3152A_11_1 (O-11_1r, U-11.1)	4.9	681	
20060919@52.asc	Broecker-1_3152A_13_1 (O-13_1r, U-13.1)	4.1	669	
20060919@53.asc	Broecker-1_3152A_15_1 (O-15_1r, U-15.1)	4.7	679	
20060919@54.asc	Broecker-1_3152A_17_1 (close to O-17_1r, U-17.1)	13.4	767	
20060919@55.asc	Broecker-1_3152A_18_1 (O-18_1c, U-18.1)	6.0	698	

Electronic supplementary material S3. Titanium concentrations in zircons analyzed by SIMS.

Ti-in-zircon temperatures were estimated based on the calibration of Watson and Harrison (2005) and Watson et al. (2006). For mounts (Broecker 1 & 3), Au-coat removed after O-analysis so that O-pits may be contaminated in Ti. The classification of zircons in jadeitite from Osayama, Japan (type I vs. type II) is after Tsujimori et al. (2005).

Filename	mount_sample_grain_no	Ti ppm	T (Ti-in-zircon), °C	Remarks
20060919@56.asc	Broecker-1_CZ3_1_1	4.9	682	standard
20060919@57.asc	Broecker-1_KIM-5, new surface	4.2	671	standard
20060919@58.asc	Broecker-3_KIM-5, new surface	4.4	674	standard
20060919@59.asc	Broecker-3_KIM-5, overlap O-pit (O-255)	4.1	668	standard
20060919@60.asc	Broecker-3_3149_7_1 (O-7_1c, U-7.1): no inclusions?	16.1	785	
20060919@61.asc	Broecker-3_3149_10_1 (O-10_1c, U-10.1)	11.2	751	
20060919@62.asc	Broecker-3_3149_15_1 (O-15_1r, U-15.1)	3.3	652	
20060919@63.asc	Broecker-3_3149_17_1 (O-17_1c, U-17.1)	5.1	685	
20060919@64.asc	Broecker-3_3149_18_1 (O-18_1r, U-18.1)	4.0	666	
20060919@65.asc	Broecker-3_3149_19_1 (O-19_1c, U-19.1)	9.3	735	
20060919@66.asc	Broecker-3_3149_32B_1 (O-32B_1r, U-32B.1)	7.2	713	
20060919@67.asc	Broecker-3_3149_32B_2 (O-32B_2c)	12.3	760	
20060919@68.asc	Broecker-3_3151_6_1 (O-6_2r, U-6.1)	6.2	700	
20060919@69.asc	Broecker-3_3151_6_2 (O-6_1c, U-6.2): no inclusions?	6.5	705	
20060919@70.asc	Broecker-3_3151_7_1 (O-7_1c, U-7.1)	11.7	755	
20060919@71.asc	Broecker-3_3151_7_2 (O-7_2r, U-7.2)	12.9	764	
20060919@72.asc	Broecker-3_3151_9_1 (O-9_1c, U-9.1)	11.5	754	
20060919@73.asc	Broecker-3_3151_16A_1 (O-16A_1c, U-16A.1)	8.7	729	
20060919@74.asc	Broecker-3_3151_16A_2 (O-16A_2r, U-16A.2)	6.4	703	
20060919@75.asc	Broecker-3_3151_17_1 (O-17_1r, U-17.1): no inclusions?	6.6	706	
20060919@76.asc	Broecker-3_3151_20_1 (O-20_1c/r, U-20.1)	8.6	728	
20060919@77.asc	Broecker-3_3151_20_2 (O-20_2c/r, U-20.2)	9.8	740	
20060919@78.asc	Broecker-3_KIM-5, overlap O-pit (O-254)	4.2	671	standard
20060919@79.asc	Broecker-3_3152B_3_1 (O-3_1c/r, U-3.1)	8.3	725	
20060919@80.asc	Broecker-3_3152B_4A_1 (O-4A_1c, U-4A.1)	9.3	735	
20060919@81.asc	Broecker-3_3152B_4A_2 (O-4A_2r, U-4A.2): no inclusions?	9.1	733	
20060919@82.asc	Broecker-3_3152B_7_1 (O-7_1r, U-7.1)	4.0	666	
20060919@83.asc	Broecker-3_3152B_7_2 (O-7_2c, U-7.2)	8.6	728	
20060919@84.asc	Broecker-3_3152B_9B_1 (O-9B_1c, U-9B.1)	5.5	691	
20060919@85.asc	Broecker-3_3152B_9_1 (O-9_1c, U-9.1)	6.1	699	
20060919@86.asc	Broecker-3_3152B_9_2 (O-9_2c/r, U-9.2)	7.6	717	
20060919@87.asc	Broecker-3_3152B_12_1 (O-12_1c/r, U-12.1)	12.4	760	
20060919@88.asc	Broecker-3_3152B_16_1 (O-16_1c, U-16.1)	5.1	685	
20060919@89.asc	Broecker-3_KIM-5, new surface	4.4	673	standard

References:

- Tsujimori T, Liou JG, Wooden J, Miyamoto T (2005) U-Pb dating of large zircons in low-temperature jadeitite from the Osayama serpentinite mélange, SW Japan: insights into the timing of serpentinization. *Int Geol Rev* 47: 1048–1057
- Watson EB, Harrison TM (2005) Zircon thermometer reveals minimum melting conditions on earliest Earth. *Science* 308: 841–844
- Watson EB, Wark DA, Thomas JB (2006) Crystallization thermometers for zircon and rutile. *Contrib Mineral Petrol* 151: 413–433

Electronic supplementary material S4. Titanium and REE concentrations (ppm) in zircons analyzed by SIMS.

Filename	mount_sample	grain_no	P	Ti	T (Ti)-in-zircon), °C														
					Y	La	Ce	Pr	Nd	Sm	Eu	Gd	Tb	Dy	Ho	Er	Tm	Yb	Lu
20051117@54.asc	Okayama, SW Japan	Tsujimori_OSI_#11_1C (U-3)	3.2	649	671	0.033	22.07	0.149	2.08	2.92	1.15	10.59	4.28	51.4	20.6	92.0	21.3	195.5	39.2
20051117@56.asc		Tsujimori_OSI_#15_1C (U-38)	1.2	583	785	0.028	12.49	0.085	0.55	1.52	0.71	6.24	3.46	49.4	21.6	118.5	31.0	323.8	72.2
20051117@55.asc		Tsujimori_OSI_#11_2R (U-5)	6.4	703	118	0.172	2.21	0.042	0.15	0.46	0.38	1.69	0.77	7.1	3.1	15.5	3.6	31.7	7.7
20051117@57.asc		Tsujimori_OSI_#5_1C (U-9)	6.3	702	278	0.020	1.10	0.030	0.53	1.03	0.48	5.01	1.75	21.0	7.2	36.4	8.4	85.5	21.5
20051117@58.asc		Tsujimori_OSI_#5_2R (U-13)	7.6	717	208	0.019	1.13	0.014	0.37	0.78	0.41	4.06	1.24	15.7	5.7	25.7	6.1	63.4	13.6
20051117@59.asc		Tsujimori_OSI_#9_1C (U-20)	2.2	623	428	0.014	4.67	0.043	0.49	1.02	0.57	5.03	2.08	26.9	12.0	62.2	16.0	169.3	41.8
	Guatemala																		
20070130@31.asc		WF018_MVE02-8-6_Zrc3_1	2210	7.8	720	0.022	2.21	0.054	0.94	3.44	0.25	37.26	22.27	318.9	130.7	654.3	171.5	1894.6	416.6
20070130@32.asc		WF018_MVE02-8-6_Zrc2_1	967	10.4	744	0.330	195.58	3.120	37.73	42.23	11.52	151.95	47.02	458.6	146.5	574.4	112.2	969.0	200.4
20070130@34.asc		WF018_MVE02-8-6_Zrc1_1	1261	17.0	790	0.008	24.72	0.141	1.79	8.46	3.41	71.27	27.32	346.5	145.0	676.4	154.3	1487.2	354.2
20070130@35.asc		WF018_MVE02-8-6_Zrc6_1	2426	12.3	8630	0.079	38.68	0.246	5.65	12.86	4.84	83.40	34.50	504.7	243.0	1319.5	310.6	3126.0	712.2
20070130@36.asc		WF018_MVE02-8-6_Zrc5_1	1365	19.4	803	0.003	32.95	0.132	2.41	7.98	3.71	81.25	32.18	448.2	186.1	893.3	195.3	1832.9	440.8
	Kimberlite (KIM-5)																		
20051117@53.asc		Tsujimori_KIM-5N	4.9	682	48	0.022	1.19	0.024	0.13	0.30	0.16	1.23	0.48	5.2	1.3	5.8	1.1	9.0	2.0
20070130@33.asc		WF018_KIM-5A	4.7	679	24	0.002	0.79	0.006	0.07	0.21	0.12	0.73	0.29	2.5	0.7	3.2	0.5	4.1	0.8
20051117@60.asc		ODP Leg 153 Gabbro (a) KIM5	12.1	758	14	0.025	0.72	0.014	0.12	0.09	0.09	0.20	0.18	1.8	0.4	1.4	0.3	2.9	0.3
20051117@72.asc		ODP Leg 153 Gabbro (b) KIM5	11.0	749	36	1.149	2.50	0.188	0.52	0.21	0.15	0.88	0.32	3.9	1.2	4.1	0.8	6.3	1.3
average (n=4)		KIM-5	8.2	717	30	0.299	1.30	0.058	0.21	0.20	0.131	0.76	0.32	3.3	0.9	3.6	0.7	5.6	1.1
1SD			3.9	42	15	0.566	0.83	0.087	0.21	0.09	0.035	0.43	0.12	1.5	0.4	1.8	0.3	2.7	0.7

Ti-in-zircon temperatures were estimated based on the calibration of Watson and Harrison (2005) and Watson et al. (2006).

This analysis only counts 3-4 out of 5 cycles due to primary beam relocation.

Zircon Th, U and 207Pb/206Pb ages, for the Okayama jadeite, after (Tsujimori et al. 2005).

Ce/Ce* = CeN/(sqrt(LaNdPrN)). Chondrite normalizing values from McDonough and Sun (1995).

The classification of zircons in jadeite from Okayama, Japan (type I vs. type II) is after Tsujimori et al. (2005).

Data sources: (1) Cavosie et al. (2009); and this study.

References:

- Cavosie, A.I, Kira, N.T., Valley, J.W. (2009) Magmatic zircons from the Mid-Atlantic Ridge: primitive oxygen isotope signature. *Am Mineral* 94, 926-934
- McDonough, W.F., Sun S.-s. (1995) The composition of the Earth. *Chem Geol* 120: 223-253
- Tsujimori T., Liou J.G., Wooden J., Miyamoto T. (2005) U-Pb dating of large zircons in low-temperature jadeite from the Okayama serpentinite melange, SW Japan: insights into the timing of serpentinization. *Int Geol Rev* 47: 1048-1057
- Watson EB, Harrison TM (2005) Zircon thermometer reveals minimum melting conditions on earliest Earth. *Science* 308: 841-844
- Watson EB, Wark DA, Thomas JB (2006) Crystalization thermometers for zircon and rutile. *Contrib Mineral Petrol* 151: 413-433

Electronic supplementary material S4. Titanium and F

Filename	mount_sample	grain_no	REE (La to Lu) Total		HF	U#	Th#	Th/U#	Th/U# (#1std, Ma)	207/206Pb age#		Ce/Ce* (Sm/La) _N	(Yb/Sm) _N	(Yb/Gd) _N	Eu/Eu*	Remarks
			U/Yb	Y/Ho												
20051117@54.asc	Okayama, SW Japan	Tsujimori_OSI_#11_1C (U-3)	463	5828	85.17	67.99	0.82	526.9±9.8	0.436	32.62	77	144	61	23	0.63	ig-type (type 11)
20051117@56.asc		Tsujimori_OSI_#15_1C (U-38)	642	7074	83.68	61.77	0.76	506.1±9.6	0.258	36.3	62	86	196	64	0.71	ig-type (type 11)
20051117@55.asc		Tsujimori_OSI_#11_2R (U-5)	75	9279	17.31	3.58	0.21	490±15.7	0.546	38.26	6	4	63	23	1.30	h-type (type 1)
20051117@57.asc		Tsujimori_OSI_#5_1C (U-9)	190	9197	12.44	2.81	0.23	523.9±18.5	0.145	38.46	11	82	76	21	0.64	h-type (type 1)
20051117@58.asc		Tsujimori_OSI_#5_2R (U-13)	138	8535	12.45	3.35	0.28	452.8±18.8	0.196	36.37	17	64	75	19	0.70	h-type (type 1)
20051117@59.asc		Tsujimori_OSI_#9_1C (U-20)	342	8104	58.53	19.94	0.35	455.7±10.1	0.346	35.76	46	120	152	42	0.76	h-type (type 1)
20070130@31.asc	Guatemala	WF018_MVE02-8-6_Zrc3_1	3653	18586	435.0	17.9	0.04		0.23	35.85	15	246	507	63	0.07	
20070130@32.asc		WF018_MVE02-8-6_Zrc2_1	2951	14527	2293.5	5895.2	2.57		2.37	34.2	47	205	21	8	0.44	
20070130@34.asc		WF018_MVE02-8-6_Zrc1_1	3301	10337	119.3	103.4	0.87		0.08	33.65	181	1749	162	26	0.42	
20070130@35.asc		WF018_MVE02-8-6_Zrc6_1	6396	8268	347.3	166.4	0.48		0.11	35.52	67	259	223	46	0.45	
20070130@36.asc	Kimberlite (KIM-5)	WF018_MVE02-8-6_Zrc5_1	4157	11466	149.2	138.5	0.93		0.08	32.57	409	4461	211	28	0.44	
20051117@53.asc		Tsujimori_KIM-5N	28	9117						36.0	12	21	28	9	0.83	
20070130@33.asc		WF018_KIM-5A	14	9374	5.0	1.1	0.23		1.211	33.16	65	221	18	7	0.96	ref (1)
20051117@60.asc		ODP Leg 153 Gabbro (a) KIM5	9	8917						31.75	9	6	30	18	1.93	
20051117@72.asc		ODP Leg 153 Gabbro (b) KIM5	24	9049						29.0	1	0.3	28	9	1.07	
average (n=4)		KIM-5	18	9114						32	22	62	26	11	1.20	
1SD			9	192						3	29	106	6	5	0.50	

Ti-in-zircon temperatures were estimated based on the calibrati
 \$ This analysis only counts 3-4 out of 5 cycles due to primary bi
 # Zircon Th, U and 207Pb/206Pb ages, for the Okayama jadeitit
 Ce/Ce* = CeN/(sqrt(LanPrN)). Chronrite normalizing values fr
 The classification of zircons in jadeitite from Osayama, Japan (t
 Data sources: (1) Cavosie et al. (2009); and this study.

References:

Cavosie, AJ, Kia NT, Valley JW (2009) Magmatic zircons from the Mid-Atlantic
 McDonough WF, Sun S-s (1995) The composition of the Earth. Chem Geol 120:
 Tsujimori T, Liou JG, Wooden J, Miyamoto T (2005) U-Pb dating of large zircon
 Watson EB, Harrison TM (2005) Zircon thermometer reveals minimum n
 Watson EB, Wark DA, Thomas JB (2006) Crystallization thermometers for zirc

